Guanidine Donors in Nonlinear Optical Chromophores

Nicholas D. Buker

A dissertation submitted in partial fulfillment of the
requirements for the degree of:

Doctor of Philosophy

University of Washington

2006

Program Authorized to Offer Degree: Department of Chemistry

University of Washington
Graduate School

This is to certify that I have examined this copy of a doctoral dissertation by

Nicholas D. Buker

and have found that it is complete and satisfactory in all respects,
and that any and all revisions required by the final
examining committee have been made.

Chair of Supervisory Committee:

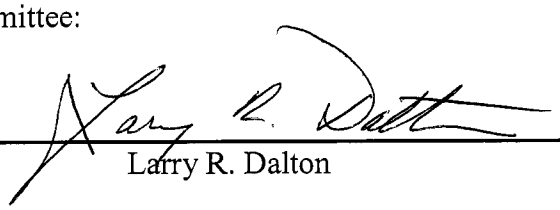

Larry R. Dalton

Reading Committee:

Larry R. Dalton

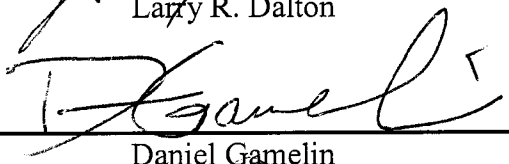

Daniel Gamelin

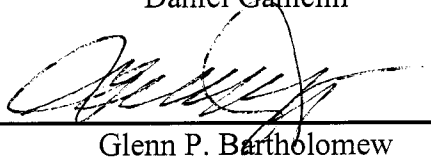

Glenn P. Bartholomew

Date: 2/15/06

In presenting this dissertation in partial fulfillment of the requirements for the doctoral degree at the University of Washington, I agree that the Library shall make its copies freely available for inspection. I further agree that extensive copying of the dissertation is allowable only for scholarly purposes, consistent with "fair use" as prescribed in the U.S. Copyright Law. Requests for copying or reproduction of this dissertation may be referred to Proquest Information and Learning, 300 North Zeeb Road, Ann Arbor, MI 48106-1346, 1-800-521-0600, to whom the author has granted "the right to reproduce and sell (a) copies of the manuscript in microform and/or (b) printed copies of the manuscript made from microform."

Signature 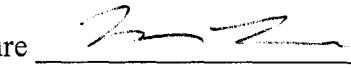

Date 03/15/06

University of Washington

Abstract

Guanidine Donors in Nonlinear Optical Chromophores

Nicholas D. Buker

Chairperson of the Supervisory Committee:
Professor Larry R. Dalton
Department of Chemistry

The variable refractive index of electro-optic (EO) materials has led to a great deal of research interest. Application of an electric field to EO materials leads to a linear variance in refractive index known as Pockel's effect. When incorporated into devices, these materials serve as an effective vehicle for rapid modulation of optical signals using electrical inputs. Nonlinear optical (NLO) chromophores are the most successful family of organic EO materials. These chromophores are typically comprised of a delocalized π-electron system that connects electron rich moieties (donors) to electron deficient functionalities (acceptors). Hyperpolarizability (β) is the component of molecular NLO behavior that is responsible for EO effects. Optimization of NLO chromophores for use in EO materials has proven to be a challenging task because enhancement of β typically results in reduced stability, decreased transparency to telecommunication wavelengths and other unwanted consequences.

A family of NLO chromophores has been synthesized containing novel donor systems based on functionalized guanidines. Some chromophores utilizing these donor systems display larger hyperpolarizabilities than those incorporating conventional donors, yet possess superior transparency and stability properties. The unusual and highly desirable characteristics of these chromophores make them very promising candidates for EO applications.

Table of Contents

List of Figures

List of Tables

Acknowledgements

I'd like to acknowledge all the members of the Dalton group, past and present who made this possible. Without their advice, insight, wisdom, friendship and patience I never would have succeeded. Additionally, I very much appreciate the time my committee members invested into this process. I'd like to thank everyone who quietly worked to support the Dalton group by taking care of countless details. Finally I'd like to thank Larry Dalton for fiercely supporting his students.

Dedication

This work is dedicated to my parents for everything they've done for me.

Chapter 1 – Introduction to Electro-Optic Materials

Section 1: Electro-Optics

The variable refractive index of electro-optic (EO) materials has led to a great deal of research interest.[1-6] Application of an electric field to EO materials leads to a linear variance in refractive index known as Pockel's effect. When incorporated into devices, these materials serve as an effective vehicle for modulation of optical signals using electrical inputs. The telecommunications industry has long exploited EO devices for satellite and fiber optic communication, but material enhancement could realize a great number of potential information handling and processing applications.[1,7-12]

A number of systems have been developed to allow modulation of optical signals including liquid crystals, electro-absorptives and EO materials. Liquid crystals work extremely well for modulating optical signals, but their slow millisecond switching time precludes their use for many applications.[1,3,5] Electro-absorpative materials such as gallium arsenide, work by tuning optical absorption with electric field. Shifting of the absorption peak with electric field allows one to control the transparency of the medium to optical signals such that they may be turned on and off. However, several problems exist with gallium arsenide systems including large optical loss and relatively high voltage requirements. EO materials possess switching times on the order of

femtoseconds enabling to them to handle much more data per time span than liquid crystals. Additionally, EO materials may be tuned so that they have superior transparency to electro-absorptive materials in conjunction with lower voltage requirements.[1,3,5]

A number of commercial devices employ a material known as lithium niobate, which is the most successful inorganic EO material. While these devices work extremely well, they have a number of drawbacks compared to organic systems. Devices based on lithium niobate have higher voltage requirements and are significantly more difficult to fabricate than organic based devices. Organic EO materials are typically incorporated into polymer or dendrimer systems that are amenable to a number of established semiconductor production techniques including spin-casting and reactive ion etching. This allows for the possibility of easy and inexpensive device fabrication and integration into modern electronics. Lithium niobate devices must be fabricated from crystals, making them difficult to produce, integrate and couple to electrodes and optical fibers. Besides being difficult to generate, the connections between lithium niobate crystals and fiber optic lines are prone to damage resulting in fragile devices. The characteristics of lithium niobate cannot be further improved due to its nature as an inorganic crystal, but organic EO chromophore systems already exceed its performance and continue to improve through modification of chromophores, polymers and fabrication

techniques.[1,3,5,7,8,10-12] Although lithium niobate has lower optical loss, organic EO materials demonstrate acceptable values and continue to improve.

Section 2: Mach-Zender Interferometer

The Mach-Zender interferometer (Figure 1.1) is perhaps the most commonly used EO device. This interferometer functions by splitting an incoming light signal into two separate arms containing EO material. In the absence of an electric field, the optical signals recombine constructively. However, when an electric field applied to one arm, the result is a voltage-controlled refractive index change, which results in a phase mismatch and destructive interference when the signals from the arms are recombined. Using this type of device one may encode a binary electrical signal into an optical one. Phase retardation by the electric field can be expressed as Equation 1.1.[5]

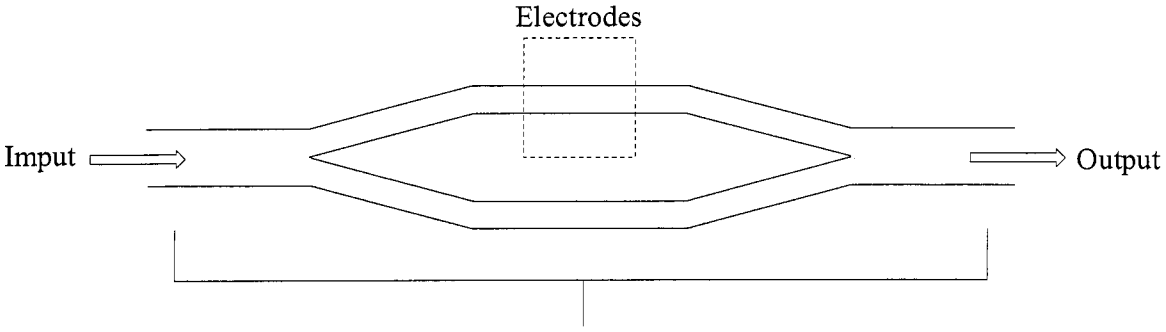

Figure 1.1 Mach-Zender interferometer

$$\Delta\phi = \frac{2\pi\Delta nL}{\lambda} = \frac{\pi n^3 r_{33} EL}{\lambda}$$ **Equation 1.1**

In this expression, Δn represents the change in refractive index of the EO material, L is the modulation length, r_{33} electro-optic coefficient of the material, E is the applied field and λ is the wavelength of light being modulated. The voltage needed by a device to achieve a phase shift of π is known as the V_π and is described in Equation 1.2 where the distance between electrodes is represented by h. It is desirable to generate devices with very low V_π in order to achieve operating voltages small enough to be compatible with integration into modern low-voltage electronic devices.[5]

$$V_\pi = \frac{\lambda h}{n^3 r_{33} L}$$ **Equation 1.2**

Section 3: The Electro-Optic Coefficient and Hyperpolarizability

Examination of Equations 1.1 and 1.2 reveals that device performance is proportional to the electro-optic coefficient. Simply put, r_{33} is the figure of merit describing the degree to which the refractive index of a material shifts upon application an electric field. Equation 1.3 describes r_{33}, where N represents the chromophore number density, F describes the electrostatic environment around the chromophore which partially shields the chromophore molecules from applied fields, β is the

hyperpolarizability, $\langle\cos^3\theta\rangle$ is the order parameter, describing the degree of acentric order, and n^4 is the fourth power of the refractive index. Hyperpolarizability is a molecular figure of merit indicating potency of a molecule for EO applications.

$$r_{33} = \frac{2NF\beta\left(\cos^3\theta\right)}{n^4} \quad \textbf{Equation 1.3}$$

EO materials are one type of a broader family of nonlinear optical (NLO) materials. Equation 1.3 indicates that r_{33} is dependent on β and chromophore orientation $\langle\cos^3\theta\rangle$. Equation 1.4 is derived from Maxwell's equations describing the interactions of electromagnetic fields which matter, expresses molecular polarizability and β is the coefficient of the second term in the expansion. Similarly, macroscopic polarizability is described in Equation 1.5 where the term $\chi^{(2)}_{ijk}$ is responsible for EO behavior.[11,12] The relationship between this coefficient and the r_{33} is described in Equation 1.6.

Microscopic: $p_i = \alpha_{ij}E_j + \beta_{ijk}E_jE_k + \gamma_{ijkl}E_jE_kE_l + \ldots$ **Equation 1.4**

Macroscopic: $P_i = \chi^{(1)}{}_{ij}E_j + \chi^{(2)}{}_{ijk}E_jE_k + \chi^{(3)}{}_{ijkl}E_jE_kE_l + \ldots$ **Equation 1.5**

$$r_{33} = \left|\frac{2\chi^{(2)}{}_{zzz}}{n^4}\right| \quad \textbf{Equation 1.6}$$

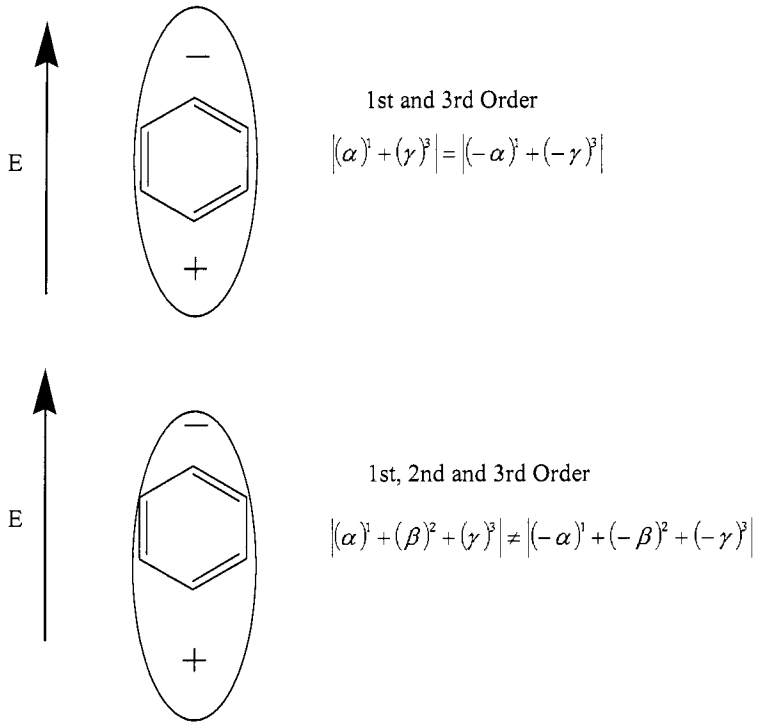

Figure 1.2 Prasad's explanation of symmetry requirements

The fact that these coefficients are second order terms in the expansions has important symmetry implications. Consider Prasad's example of benzene under an applied potential as shown in Figure 1.2.[11] The application of a potential to a highly symmetrical molecule, such as benzene, results in an induced dipole that is positive in one direction and negative in the opposite direction with the positive and negative components being of equal magnitude. Figure 1.2 illustrates that the first and third terms

from the expansion 1.4 cancel and thus charge is conserved. However, when the second term is introduced to the equation, sign is lost because it is squared. Consequently, addition of the first, second and third terms of the expansion, the magnitudes of charge are no longer equal. This result is illogical for a symmetrical molecule such as benzene and implies that charge is not conserved. Therefore, even terms are disallowed from having nonzero values in expansions describing polarizability along an axis of symmetry.[11] Figure 1.3 depicts the microscopic implications of this fact, where the stilbene molecule that is symmetric along its long axis is forbidden from having non-zero β non-zero along this axis, while the asymmetrically functionalized stilbene possesses a non-zero β along its long axis.

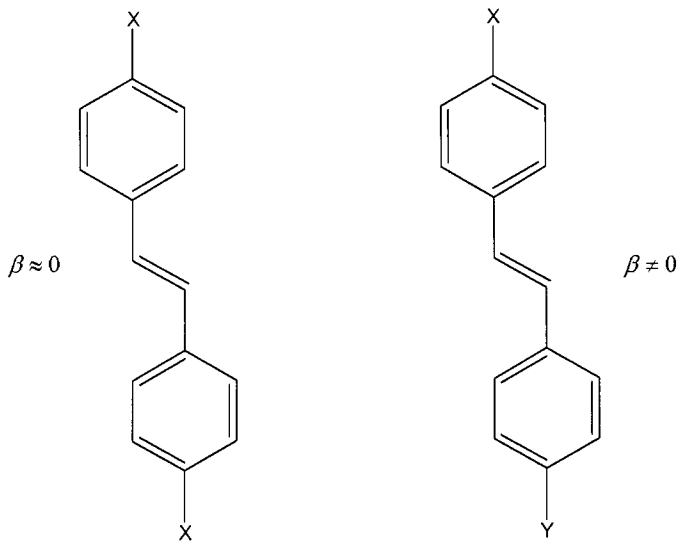

Figure 1.3 Symmetric and asymmetric stilbene molecules

The mathematical arguments that dictate molecular asymmetry can be extended to macroscopic systems. In order for material to possess EO activity, it is necessary for the chromophores to possess net orientation in a similar direction and consequently inducing an overall asymmetry in the material. The higher the degree to which chromophores are oriented in the same direction, the higher EO activity will be observed because more translation β to the macroscopic property r_{33} will be observed. The $<\cos^3\theta>$ portion of Equation 1.3 describes the degree to which asymmetry is achieved in a bulk material and is illustrated in Figure 1.4.[5,11]

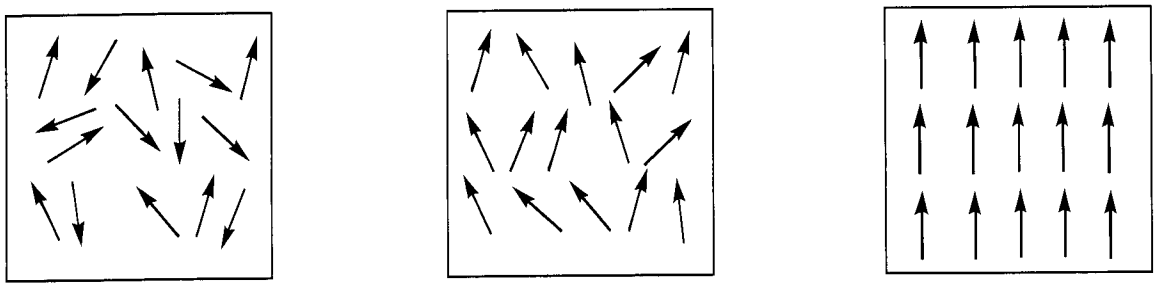

$\cos^3\theta \approx 0$ $\quad 0 < \cos^3\theta < 1$ $\quad \cos^3\theta \approx 1$

Figure 1.4 Schematics of chromophore orientation and order parameter

Section 4: Achieving Order in EO Materials

One of the greatest challenges in the field of electo-optics is effective translation of molecular β to macroscopic r_{33}.[1,5,7,8] The asymmetric nature of these molecules results in a sizable dipole moment and consequently significant electrostatic interaction between the molecules. Figure 1.4 illustrates various degrees of acentric order in an EO material. The first frame is representative of an EO sample where molecular orientation is controlled by two factors: entropic randomization and electrostatic interactions. Although these forces are in competition with each other (entropy striving for randomness and electrostatic interactions towards centrosymmetric order) both of them work against realization of the acentric order required for bulk EO behavior to be observed. Special steps must be taken to overcome these forces in order to drive the system towards the acentricity illustrated in the second and third frames.

Although an array of techniques have been employed to generate acentric order in EO materials, they can be grouped into two categories. The first group of techniques utilize application of an external force to induce acentric order and shall be referred to as poling methods. This external force may be electrical, magnetic or optical in nature, but use electrical forces are by far the most common and hence forth the term poling will be used to describe use electrical poling.[13,14] The poling technique requires only that

chromophores have a dipole moment and lack mobile ions making it applicable to the vast majority of systems. The second group of methods rely upon internal forces to create acentric order and shall be referred to as self-assembly techniques. Sequential synthesis and crystallization are two self-assembly techniques that have been employed to create high degrees of acentric order, but self-assembly techniques are applicable to a relatively small group of systems due to the specialized molecules required.[15-17] The research discussed in this treatise involves only poling.

Section 5: EO Material Optimization

Traditionally acentric order has been induced by dispersing the chromophores in a polymer matrix and by heating the system to its glass transition temperature while applying an electric poling field. This field aligns the chromophore molecules such that partial acentric order in generated. Once the material has cooled the electric field may be turned off and the polymer matrix will lock the order by restricting chromophore mobility. A number of techniques have been employed to increase the value of r_{33} achieved as well as enhancing its thermal and temporal stability.

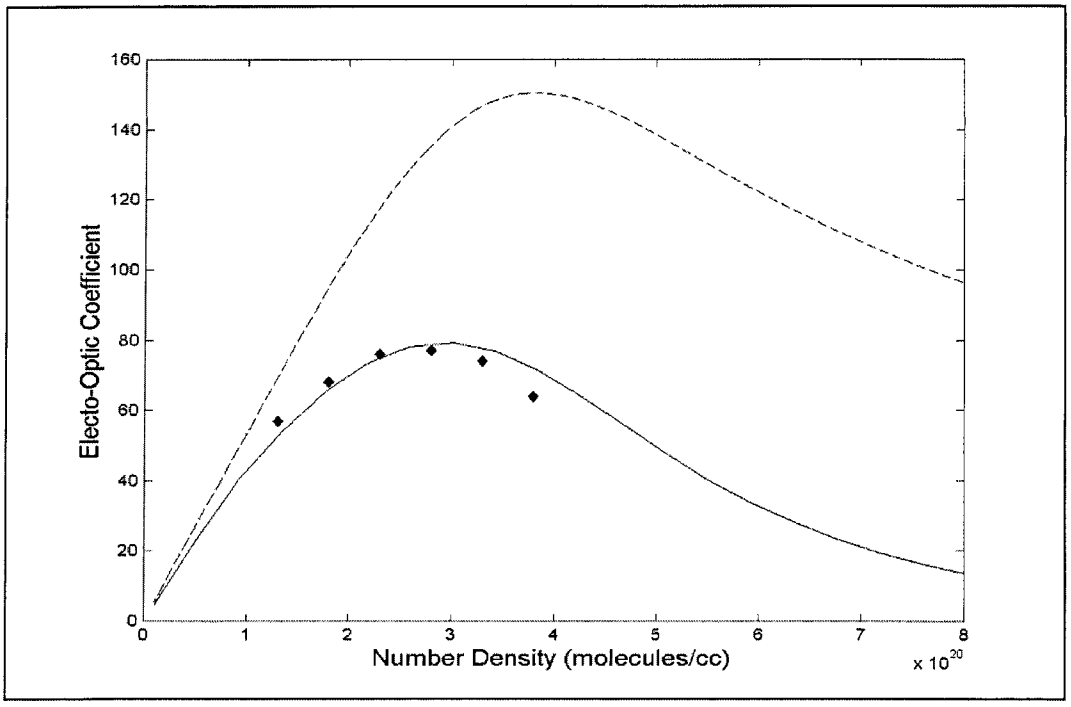

Figure 1.5 Chromophore shape and number density and roll off

Of the components contributing to r_{33} in equation 1.3, only N, β and $<cos^3\theta>$ can be readily controlled through chromophore modification. Methods for improving β will be discussed later, but enhancements to N and $<\cos^3\theta>$ are also of great importance. An obvious way to increase r_{33} is simply to increase the amount of chromophore in the polymer matrix, but problems arise when concentration rises too high and r_{33} begins to roll off. This is due to the electrostatic interactions between the chromophores. These strong interactions can be difficult to overcome even when powerful poling fields are applied.[18-20] If the chromophores are functionalized with bulky groups, the electrostatic interactions between chromophores may be reduced by increasing dipole-dipole distance,

allowing larger values of N without decreasing $<\cos^3\theta>$. This move from flat, long rod-like molecules to more spherical shapes increases solubility and poling efficiency. Figure 1.5 illustrates the increase and then subsequent decrease in r_{33} value as the chromophore concentration increases. The upper curve represents spherical chromophores while the lower curve represents rod-like chromophores. Note that data is initially linear but then rolls as chromophore-chromophore interactions become significant. Also note that the maximum attainable r_{33} value is significantly larger and occurs at higher number density for spherically shaped chromophores resulting from decreased electrostatic interactions between molecules.

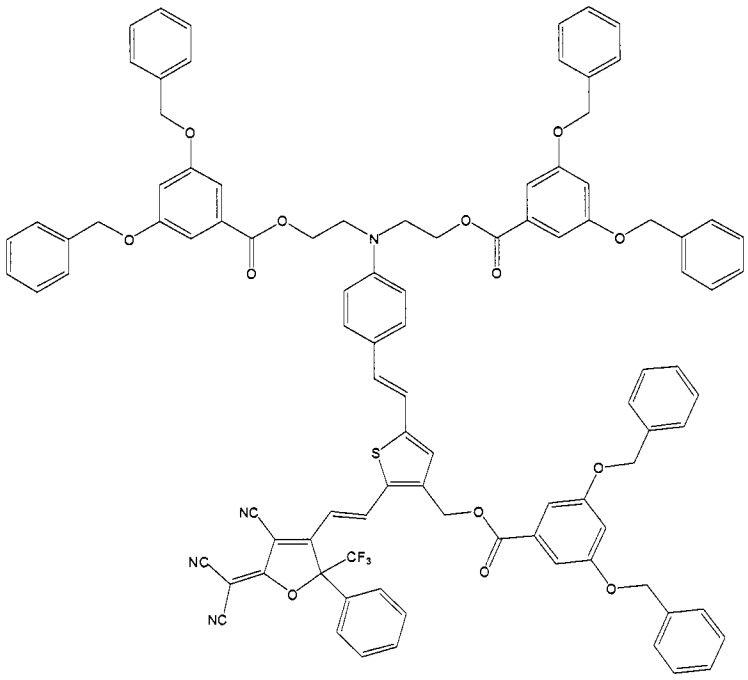

Figure 1.6 Chromophore approximating spherical shape

Figure 1.6 depicts a system with an extremely large r_{33} value in excess of 100 pm/V resulting from a high degree of functionality approximating a spherical shape. Conventional chromophores tend to crystallize necessitating the use of a polymer matrix, but these highly functionalized chromophores may be cast into glasses neat.[21-24] The addition of steric bulk is not the only important paradigm useful to designing successful EO materials. The incorporation of cross-linking agents aids in retention of activity. Cross-linking is process of bonding polymer or dendrimer molecules to each other. By linking these molecules the lattice is hardened and molecular mobility within the matrix is reduced.

The acentric order induced by the poling process is significantly higher in energy than centrosymmetric order and the system will decay over time back to the centrosymmetric state. Cooling the polymer matrix to below the glass transition temperature during the poling process will help enforce this order, but it is helpful to cross-link the system to provide a barrier to thermal randomization. Diels-Alder chemistry provides a tunable, thermally initiated and byproduct-free method for cross-linking as illustrated in Figure 1.7.[25,26]

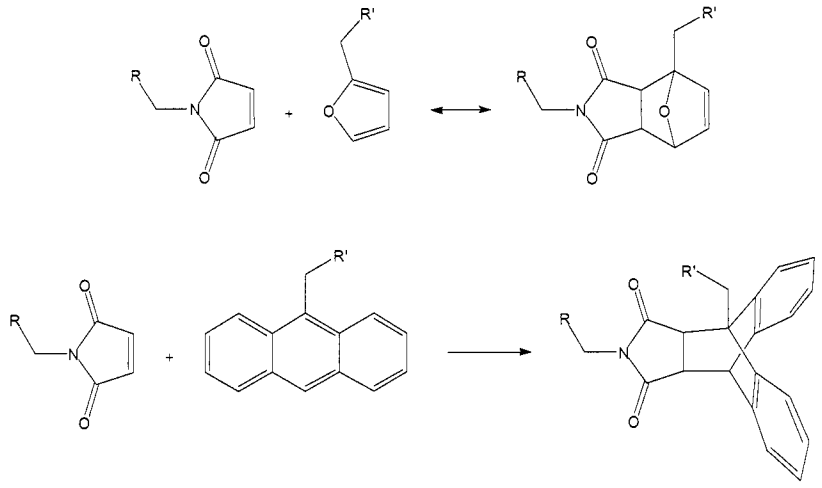

Figure 1.7 Reversible and irreversible Diels-Alder crosslinking groups

Section 6: Experimental Determination of the EO Coefficient

Figure 1.8 illustrates the simple reflection technique developed by Teng and Man which is frequently employed to measure the EO coefficient of a material.[27] A sample is prepared by casting a EO film onto an indium tin oxide (ITO)/glass slide and sputtering a gold electrode onto the film. The sample is then poled by applying a potential to the gold and ITO electrodes while heating. To measure the r_{33} of the sample, a polarized laser beam is passed through the sample at a 45-degree angle and reflected off the gold electrode. The EO film causes birefringence that manifests itself as a rotation in the polarization angle of the laser beam. After the beam exits the sample it is passed through a Soleil-Babinet compensator (a device allowing control of the polarization angle a beam of light) and a second polarizer. The Soleil-Babinet compensator is adjusted such that

light reaches the detector at or near 50% so that changes in polarization angle will result in large changes in intensity. When a potential is applied to an EO sample the degree of birefringence changes and consequently the polarization angle will vary resulting in a change in intensity observed by the detector. The dependence of intensity upon the applied voltage can be used to calculate the r_{13} of a given material, which is then multiplied by 3 to yield the r_{33} value.

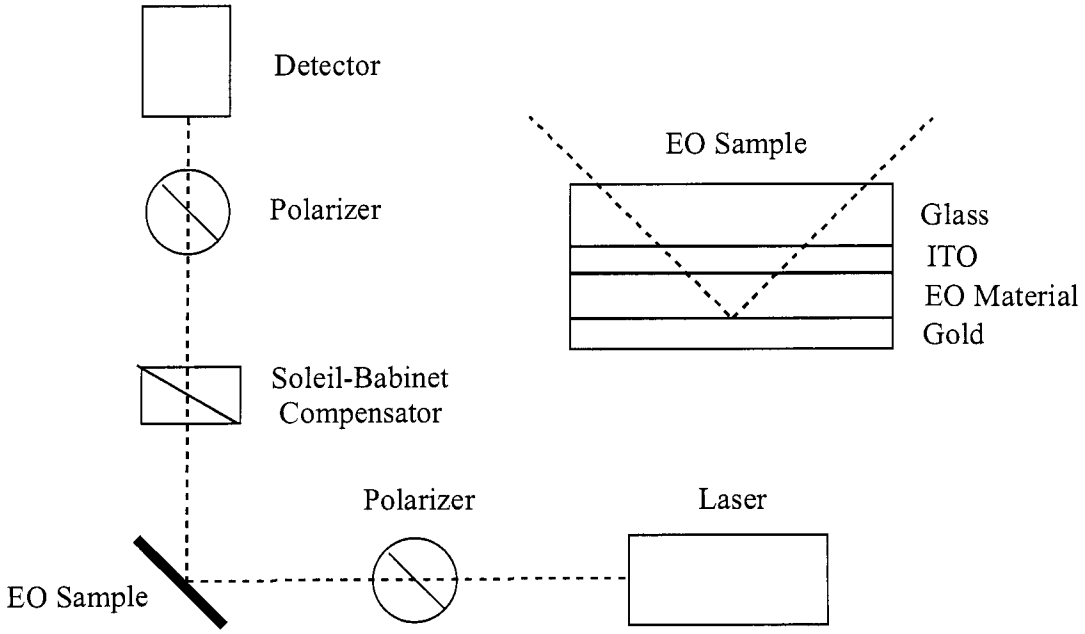

Figure 1.8 Simple reflection apparatus

Notes to Chapter 1

(1) Dalton, L. R. *Nature* **1992**, 359, 269.

(2) Ahlheim, M.; Barzoukas, M.; Besworth, P. V.; Blanchard-Desce, F. A.; Hu, Z.-Y.; Marder, S. R.; Perry, J. W.; Runser, C.; Staehelin, M.; Zysset, B. *Science* **1996**, 271, 335-337.

(3) Marder, S. R.; Perry, J. W. *Science*, **1994**, 263, 1706-1707.

(4) Marder, S. R.; Cheng, L.-P.; Tiemann, B. G.; Friedli, A. C.; Blanchard-Desce, M.; Perry, J. W.; Runser, C.; Staehelin, M.; Zysset, B. *Science*, **1994**, 263, 511-514.

(5) Dalton, L. R. *Adv. Polym. Sci.* **2002**, 158, 1-68.

(6) Marder, S. R.; Gorman, C. B.; Meyers, F.; Perry, J. W.; Bourhill, G.; Bredas, J. L.; Pierce, B. M. *Science*, **1994**, 265, 632-635.

(7) Dalton, L. R.; Sapochak, L. S.; Yu, L. *J. Phys. Chem.* **1993**, 97, 2871-2883.

(8) Dalton, L. R.; Harper, A. W.; Ghosn, R.; Steier, W.; Ziarim, M.; Fetterman, H. R.; Shi, Y.; Mustacich, R. V.; Jen, A. K.-Y.; Shea, K. J. *Chem. Mater.* **1995**, 7, 1060-1081.

(9) Franken, P. A.; Hill, A. E.; Peters, C. W.; Weinreich, G. *Phys. Rev. Lett.* **1961**, 7, 118-120.

(10) Nie, W. *Adv. Mater.* **1993**, 5, 520-545.

(11) Prasad, P. N.; Williams, D. J. *Introduction to Nonlinear Optical Effects in Molecules and Polymers*; John Wiley and Sons: New York, **1991**.

(12) Shen, Y. R. *The Principles of Nonlinear Optics*; John Wiley and Sons: New York, **1984**.

(13) Dalton, L. R.; Steier, W.; Robinson, B. H.; Zhang, C.; Ren, A.; Garner, S.; Chen, A.; Londergan, T.; Irwin, L.; Carlson, B.; Fifield, L.; Phelan, G.; Kincaid, C.; Amend, J.; Jen, A. K.-Y. *Mater. Chem.* **1999**, 9, 1905-1920.

(14) Steier, W. H.; Chen, A.; Lee, S. S.; Garner, S.; Zhang, H.; Chuyanov, V.; Dalton, L. R.; Wang, F.; Ren, A.; Zhang, C.; Todorova, G.; Harper, A. W.; Fetterman, H. R.; Chen, D.; Udupa, A.; Bhattacharya, D.; Tsap, B. *Chem. Phys.* **1999**, 245, 487-506.

(15) Bella, S.; Fragala, I.; Ratner, M. A.; Marks, T. J. In *Chem. Mater.* **1995**, 7, 400-404.

(16) van der Boom, M. E.; Zhu, P.; Evmenenko, G.; Malinsky, J. E.; Lin, W. D.; Marks, T. J. *Langmuir*, **2002**, 18, 3704-3707.

(17) van der Boom, M. E.; Evmenenko, G.; Dutta, P.; Marks, T. J. *Mater. Sci. Eng.* **2002**, 375-376.

(18) Dalton, L. R.; Harper, A. W.; Robinson, B. H. *Proc. Natl. Acad. Sci.* **1997**, 94, 4842-4847.

(19) Dalton, L. R.; Harper, A. W. *Polym. News*, **1998**, 23, 114-120.

(20) Harper, A. W.; Sun, S.; Dalton, L. R.; Garner, S. M.; Chen, A.; Kalluri, S.; Steier, W. H. *J. Opt. Soc. Am. B: Opt. Phys.* **1998**, 15, 329-337.

(21) Londergan, T.; Zhang, C.; Ren, A.; Dalton, L. R. *Polym. Prepr. (Am. Chem. Soc. Div. Polym. Chem.)* **2000**, 41, 783-784.

(22) Luo, J.; Ma, H.; Haller, M.; Jen, A. K.-Y.; Barto, R. R. *Chem. Comm.* **2002**, 888-889.

(23) Xu, C.; Wu, B.; Todorova, G.; Dalton, L. R.; Shi, Y.; Ranon, P. M.; Steier, W. H. *Macromolecules*, **1993**, 26, 5303-5309.

(24) Song, S.; Lee, S. J.; Cho, B. R. *Chem. Mater.* **1999**, 11, 1406-1408.

(25) Haller, M.; Luo, J.; Li, H.; Kim, T.-D.; Liao, Y.; Robinson, B. H.; Dalton, L. R.; Jen, A. K.-Y. *Macromolecules*, **2004**, 37, 688-690.

(26) Luo, J.; Liu, S.; Haller, M.; Liu, L.; Ma, H.; Jen, A. K.-Y. *Adv. Mater.* **2002**, 14, 1763-1768.

(27) Teng, C. C.; Man, H. T. *Appl. Phys. Lett.* **1990**, 56, 1734-1736.

Chapter 2 – Introduction to Nonlinear Optical Chromophores

Section 1: Nonlinear Optical Chromophores

Charge-transfer chromophores are the most successful family of organic EO materials.[1-3] These chromophores are comprised of a delocalized π-electron system that may be polarized under the influence of an electric field. Figure 2.1 illustrates the shifting electron density of 4-(dimethylamino)-4'-nitrostilbene (DANS) under the influence of a strong electric field. An applied electric field perturbs the ground state such that the donor transfers electron density through the π-system to the acceptor. Under the proper circumstances, this polarization change can translate into macroscopic behavior as described in Chapter 1 and is the origin of the Pockel's effect.[1-4]

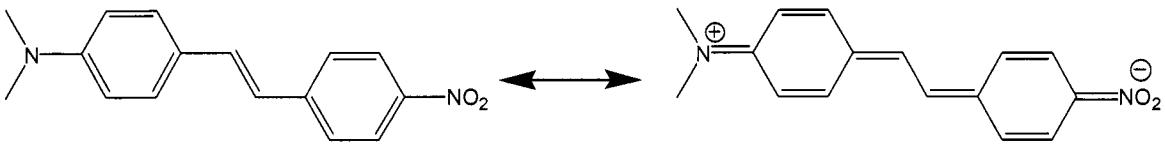

Figure 2.1 The DANS chromophore

Section 2: The Two-State Model

It can be difficult to conceptualize β, but understanding can be found by invoking the two-state model. This simplified model approximates the action of an electric field

upon a charge transfer chromophore as an electronic transition from the neutral ground to state to a charge-separated first excited state.[5-7] Although the accuracy of this model is compromised because electric field induced charge transfer in these chromophores arises from perturbation of the energy levels resulting in a new HOMO rather than a HOMO-LUMO transition, it serves as a rough qualitative representation for visualization of chromophore activity. The two-state model allows β to be represented by Equation 2.1 where μ_{ee}, μ_{gg} and μ_{ge} represent the excited, ground and transition dipole moments respectively and ΔE_{ge} is the HOMO-LUMO energy gap. Simply stated, β is dependent on the ability to shift electron density across a molecule and the energy required to do so.

$$\beta \propto \frac{(\mu_{ee} - \mu_{gg})(\mu_{ge})^2}{(\Delta E_{ge})^2} \quad \textbf{Equation 2.1}$$

The two-state model has important implications regarding molecular optimization in order to maximize β and consequently increase potential material performance. The (μ_{ee} – μ_{gg}) portion of the equation indicates that increasing the difference in dipole moment between the ground and first excited states increases β. This suggests that increasing chromophore length (distance between charges) and donor/acceptor strength (charge magnitude) will increase β. The transitional dipole moment is dependent on delocalization and its roll in this equation indicates that chromophores with large degrees of delocalization and π-orbital overlap should display large β values. The two-state

model also indicates an inverse proportionality between β and the HOMO-LUMO energy gap squared and consequently minimization of this energy results in large β values. Selection of powerful donors and acceptors in conjunction with limiting the aromaticity of bridging structures results in a decrees of the HOMO-LUMO energy gap. Experimental results correlate well to the prediction made by the two-state model and Figure 2.2 illustrate the structures of the DANS and YL-130 chromophores. The two-state model predicts that YL-130 should have a much larger β value because it is longer, has a lower degree of aromaticity in it's bridge, is highly planar and uses a much more powerful acceptor and experimental results are consistent with this.[8]

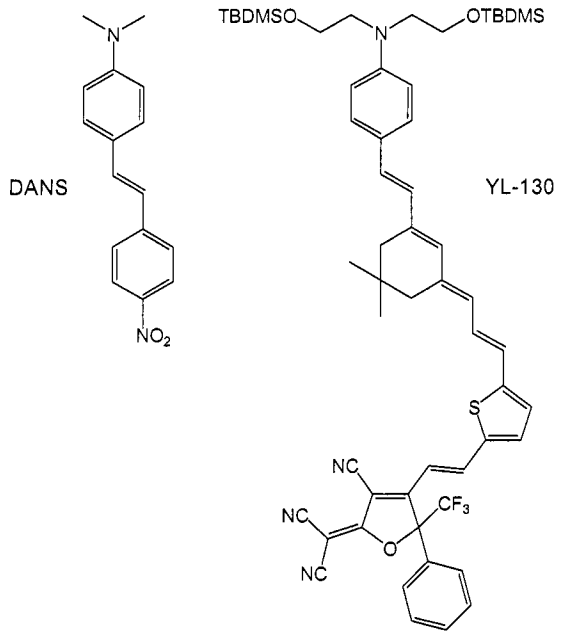

Figure 2.2 Low β chromophore vs high β chromophore

The two-state model not only serves as a conceptual aid to understand optimization of chromophore nonlinearity, but also as a tool to understand the negative effects of increasing β. To some degree, the very characteristic that result in enhanced β value, such as increased conjugation length and planarity, decreased HOMO-LUMO gap and usage of powerful acceptors, results in increased aggregation, diminished solubility, decreased stability and reduced transparency to telecommunication wavelengths.[3,9,10] While these effects can be mitigated to some degree through clever design, a balance must be struck.

Section 3: Experimental Determination of β

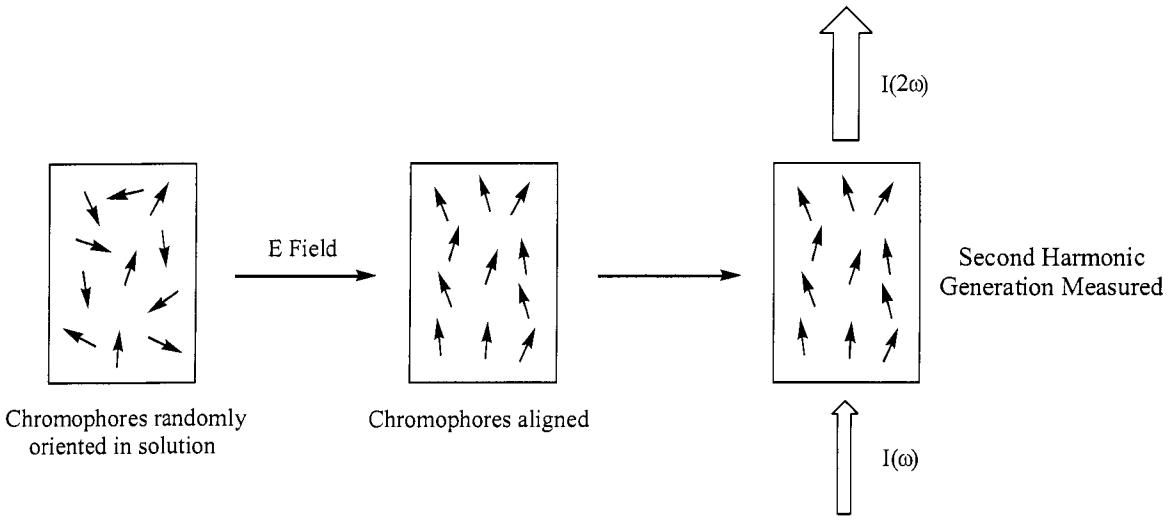

Figure 2.3 The EFISH technique

Electric-Field Induced Second-Harmonic Generation (EFISH) was one of the first methods developed to measure molecular nonlinearity. As illustrated in Figure 2.3, a solution of the NLO molecules is subjected to electric field to induce noncentrosymmetric order. The bulk ordering achieved using this method results in a relatively strong second harmonic generation. The intensity of the second harmonic signal is used to determine the quantity $(\mu\beta/5kT)+\gamma$. Although this technique has relatively simple equipment requirements compared to other techniques used to probe molecule nonlinearity, there are significant issues. EFISH requires electric field induced order and consequently is only compatible with nonionic dipolar molecules. Another issue is that EFISH does not measure β directly, but rather than quantity $(\mu\beta/5kT)+\gamma$. Disentangling the value of β from that quantity is a challenge as μ (dipole moment) is difficult to determine experimentally and environmentally dependent which complicates calculational determination. Furthermore, the contribution of γ (third order nonlinear response) to the quantity is nontrivial to determine.

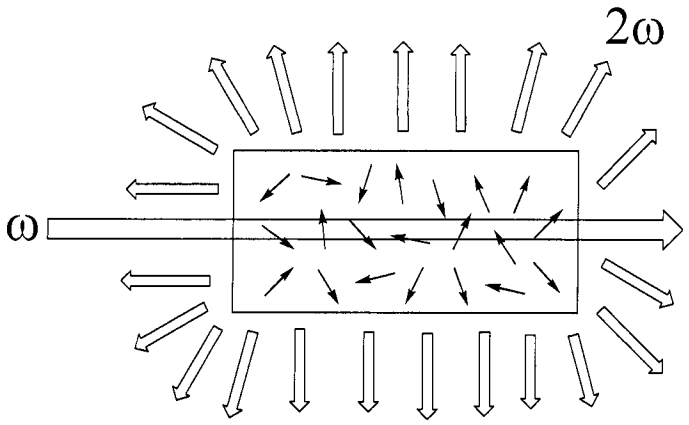

Figure 2.4 The HRS technique

Hyper-Raleigh scattering (HRS) is another technique used to test molecular nonlinearity. This technique examines nonlinear light scattering at the second harmonic frequency. HRS was first demonstrated in 1965, shortly after the advent of the laser, but it was rarely employed until the 1990's.[11-13] This technique uses two-photon elastic light scattering to determine β without entangling it with other molecular properties. HRS does not involve electric field induced order and consequently is compatible with a number of materials which EFISH is not such as those lacking dipole moment and those which possess an ionic (conductive) nature. HRS is a two-photon process in which two photons of frequency ω are annihilated and a single photon with twice the energy and half the wavelength is created (Figure 2.4).

$$I(2\omega) = G(N_{solvent} < \beta^2_{solvent} > + N_{sample} < \beta^2_{sample} >)$$ **Equation 2.2**

The relationship between the emitted 2ω light and β is described in Equation 2.2 where $I(2\omega)$ is the observed HRS signal intensity, G is an instrumental calibration factor and N is the number density of molecules in solution.[11] This direct relationship between $I(2\omega)$ and β combined with larger array of materials with which the technique compatible makes HRS a more desirable technique for determination of β than EFISH. The values reported in this treatise are relative to the β value of chloroform.[13-15]

Section 4: Modular Synthesis of Chromophores

By nature, charge transfer chromophores are generally composed of a donor, bridge and acceptor. These segments may be prepared individually and this library of donor, bridge and acceptor building blocks may be assembled into an array of chromophores. This modular synthesis of chromophores is illustrated in Figure 2.5 and allows chromophore properties to be tailored through systematic study and facilitates investigation of structure property relationships.

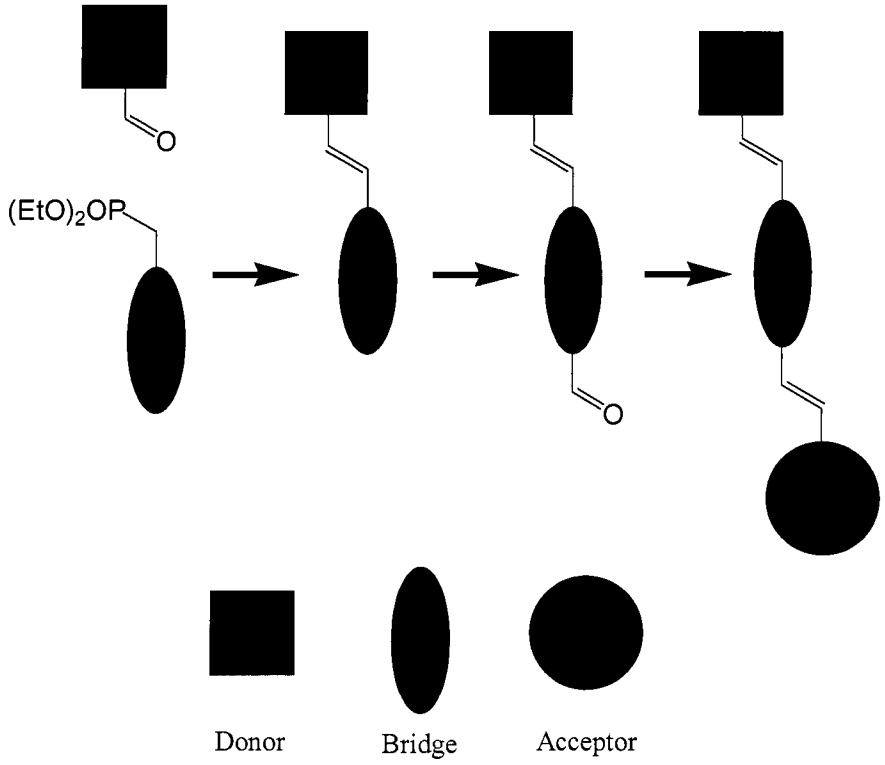

Figure 2.5 A conventional chromophore synthesis

Section 5: Optimization of β

The two-state model predicts that chromophore β will depend on the length, delocalization and strength of the donor and acceptor. This theory has correlated quite well with experimental results allowing a relatively high degree of understanding of the relationship between structures and nonlinearity.[16-22] Although various donors have been explored, nearly all reported chromophores utilize tertiary amines. Amino donors offer a combination of synthetic ease, stability and potency that has made them the standard.

Acceptors and bridges on the other hand, are highly varied and have evolved drastically over the years of NLO chromophore research.[22-34] Figure 2.6 illustrate an array of acceptors frequently found in the literature and their relative strengths. It is important to note that while usage of the most powerful acceptor generally results in the highest β value, it does not always translate well into material EO performance. Materials employing the two most power acceptors in this figure (TCP and TCNQ) generally perform worse than those containing the other two acceptors in that row (TCF and TCF-CF_3). The extreme planarity of TCP and TCNQ leads to aggregation issues resulting in chromophore-chromophore interactions reducing poling efficiency and consequently the order parameter. Additionally, the TCNQ acceptor is so powerful that chromophores containing it are generally zwitterionic which leads to purification, solubility, aggregation and transparency issues.

Weak Acceptors:

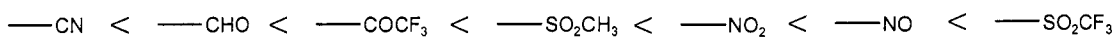

Medium Acceptors:

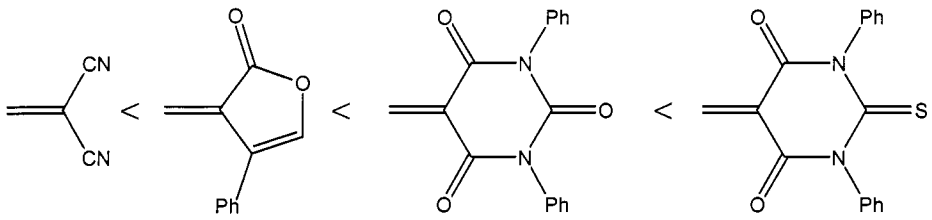

Strong Acceptors:

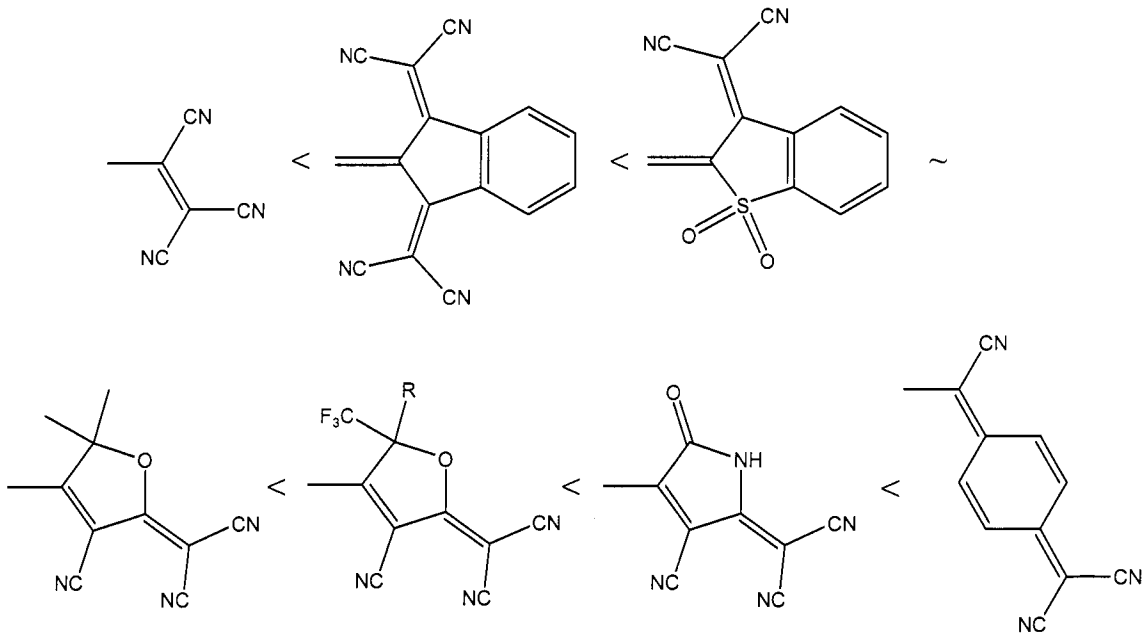

Figure 2.6 Relative acceptor strength

Bridge effectiveness is related to both its length and structure.[24-43] Generally the longer the bridge used, the higher the β value. Increased length comes at the expense of greater synthetic difficulty, decreased solubility and frequently reduced stability.[9,10]

Highly aromatic bridges are typically very stable and relatively easy to synthesize, but significantly less efficient then polyene bridges due to aromaticity hindering delocalization. Figure 2.7 illustrates a series of bridge components that may be assembled in various combinations to link donors and acceptors in NLO chromophores.

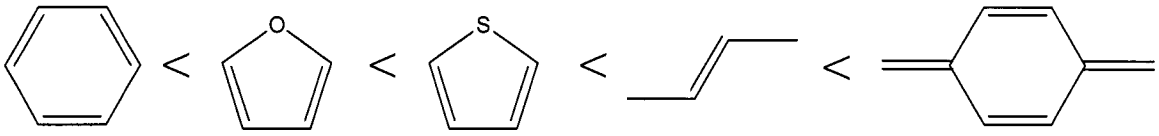

Figure 2.7 Bridge components in order of relative delocalization ability

Knowledge of the relative effectivenesses of various chromophore components can be used to predict and understand behavior. Table 2.1 illustrates the $\mu\beta$ and $\mu\beta/M_w$ of various chromophores. The value $\mu\beta/M_w$ is useful for predicting potential material performance. The quantity r_{33} is dependent on both β and number density. As chromophore size increases, maximum possible number density decreases because each chromophore occupies a larger space. The molecular weight provides a rough estimate of molecular volume and therefore $\mu\beta/M_w$ is roughly proportional to molecule nonlinearity over volume. The relative acceptor and bridge efficiencies illustrated in Figures 2.6 and 2.7 may be used to explain the trends shown in Table 2.1.[44]

Table 2.1 Comparison of structure to $\mu\beta$ and $\mu\beta/M_w$

NLO Chromophore	$\mu\beta$*	$\mu\beta/M_w$	NLO Chromophore	$\mu\beta$*	$\mu\beta/M_w$
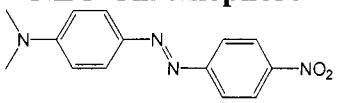	580	2.1	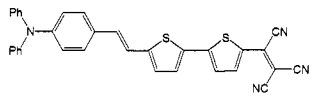	10600	19.8
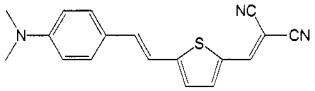	1300	3.9	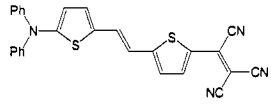	10200	22.1
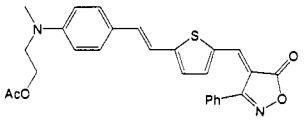	2000	4.1	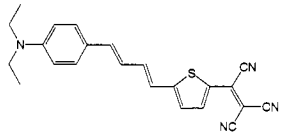	9800	25.5
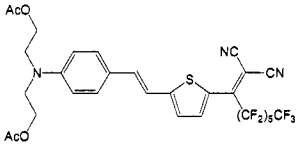	3300	4.3	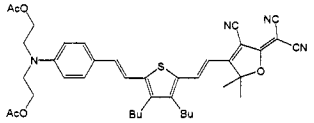	18000	25.9
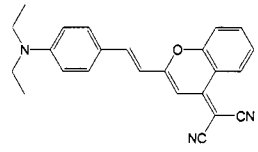	1720	4.7	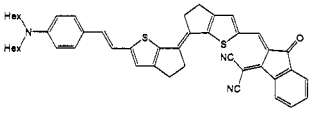	19400	26.4
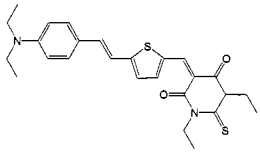	2400	5.1	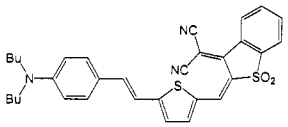	15000	27.1
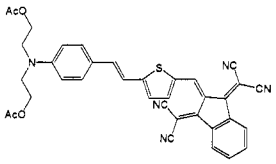	6100	9.7	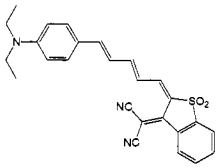	13500	27.1
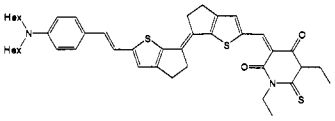	10400	14.1	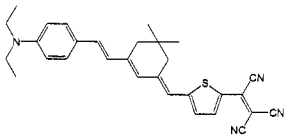	13000	27.2
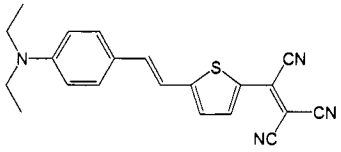	6200	17.3	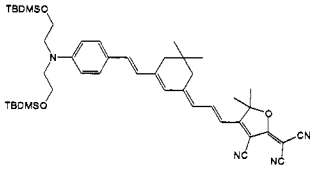	35000	45.7

*$\mu\beta$ in 10^{-48} esu at 1907nm

Notes to Chapter 2

(1) Dalton, L. R. *Nature* **1992**, 359, 269.

(2) Marder, S. R.; Perry, J. W. *Science*, **1994**, 263, 1706-1707.

(3) Dalton, L. R. *Adv. Polym. Sci.* **2002**, 158, 1-68.

(4) Prasad, P. N.; Williams, D. J. *Introduction to Nonlinear Optical Effects in Molecules and Polymers*; John Wiley and Sons: New York, **1991**.

(5) Lalama, S. J.; Garito, A. F. *Phys. Rev. A: At. Mol. Opt. Phys.* **1979**, 20, 1179-1194.

(6) Oudar, J. L.; Chemla, D. S. *J. Chem. Phys.* **1977**, 66, 2664-2668.

(7) Levine, B. F.; Bethea, C. G. *J. Chem. Phys.* **1977**, 66, 1070-1074.

(8) Firestone, K. A., personal communication

(9) Raimundo, J.-M.; Blanchard, P.; Gallego-Planas, N.; Mercier, N.; Ledoux-Rak, I.; Hierle, R.; Roncali, J. *J. Org. Chem.* **2002**, 67, 205-218.

(10) Rao, V. P.; Wong, K. Y.; Jen, A. K.-Y.; Drost, K. J. *Chem. Mater.* **1994**, 6, 2210-2212.

(11) Firestone, K. A.; Reid, P. J.; Lawson, R.; Jang, S.-H.; Dalton, L. R. *Inorg. Chim. Acta.* **2004**, 357, 3957-3966.

(12) Karna, S. P.; Zhang, Y.; Samoc, M.; Prasad, P. N.; Reinhardt, B. A.; Dillard, A. G. *J. Chem. Phys.* **1993**, 99, 9984-9993.

(13) Clays, K.; Persoons, A. *Phys. Rev. Lett.* **1991**, 66, 2980-2983.

(14) Kaatz, P.; Shelton, D. P. *Opt. Commun.* **1998**, 157, 177-181.

(15) Kazjar, F.; Ledoux-Rak, I.; Zyss, J. *Phys. Rev. A.*, **1987**, 36, 2210-2219.

(16) Marder, S. R.; Gorman, C. B.; Meyers, F.; Perry, J. W.; Bourhill, G.; Bredas, J. L.; Pierce, B. M. *Science*, **1994**, 265, 632-635.

(17) Bella, S. D.; Fragala, I.; Ratner, M. A.; Marks, T. J. *Chem. Mater.* **1995**, 7, 400-404.

(18) Bredas, J. L.; Adant, C.; Tackx, P.; Persoons, A.; Pierce, B. M. *Chem. Rev.* **1994**, 94, 243-276.

(19) Champagne, B.; Kirtman, B. *Chem. Phys.* **1999**, 245, 213-226.

(20) Lipinski, J.; Bartkowiak, W. *Chem. Phys.* **1999**, 245, 263-276.

(21) Painelli, A. *Chem. Phys.* **1999**, 245, 185-197.

(22) Tretiak, S.; Chemnyak, V.; Mukamel, S. *Chem. Phys.* **1999**, 245, 145-163.

(23) Ahlheim, M.; Barzoukas, M.; Besworth, P. V.; Blanchard-Desce, F. A.; Hu, Z.-Y.; Marder, S. R.; Perry, J. W.; Runser, C.; Staehelin, M.; Zysset, B. *Science* **1996**, 271, 335-337.

(24) Marder, S. R.; Cheng, L.-P.; Tiemann, B. G.; Friedli, A. C.; Blanchard-Desce, M.; Perry, J. W.; Runser, C.; Staehelin, M.; Zysset, B. *Science*, **1994**, 263, 511-514.

(25) Burland, D. M.; Miller, R. D.; Reiser, O.; Tweig, R. J.; Walsh, C. A. *J. Appl. Phys.* **1992**, 71, 410-417.

(26) Cheng, L.-T.; Tam, W.; Marder, S. R.; Steigman, A. E.; Rikken, G.; Spangler, C. W. *J. Phys. Chem.* **1991**, 95, 10643-10653.

(27) Cheng, L.-T.; Tam, W.; Stevenson, S. H.; Meredith, G. R.; Rikken, G.; Marder, S. R. *J. Phys. Chem.* **1991**, 10631-10643.

(28) Jen, A. K.-Y.; Rao, V. P.; Drost, K. J.; Wong, K. Y.; Cava, M. P. *J. Chem. Soc., Chem. Commun.* **1994**, 2057-2059.

(29) Jen, A. K.-Y.; Wong, K. Y.; Rao, V. P.; Drost, K. J.; Cai, Y. M. *J. Electron. Mater.* **1994**, 23, 653-657.

(30) Katz, H. E.; Singer, K. D.; Sohn, J. E.; Dirk, C. W.; King, L. A.; Gordon, H. M. *J. Amer. Chem. Soc.* **1987**, 109, 6561-6563.

(31) Moylan, C. R.; Tweig, R. J.; Vee, V. Y.; Swanson, S. A.; Betterton, K. M.; Miller, R. D. *J. Am. Chem. Soc.* **1993**, 115, 12599-12600.

(32) Rao, V. P.; Cai, Y. M.; Jen, A. K.-Y. *J. Chem. Soc., Chem. Commun.* **1994**, 1689-1690.

(33) Singer, K. D.; Sohn, J. E.; King, L. A.; Gordon, H. M.; Katz, H. E.; Dirk, C. W. *J. Opt. Soc. Am. B: Opt. Phys.* **1989**, 6, 1339-1350.

(34) Williams, D. J. *Angew. Chem. Int. Ed.* **1984**, 23, 690-703.

(35) Song, S.; Lee, S. J.; Cho, B. R. *Chem. Mater.* **1999**, 11, 1406-1408.

(36) Brasselet, S.; Cherioux, F.; Audebert, P.; Zyss, J. *Chem. Mater.* **1999**, 11, 1915-1920.

(37) Cho, B. R.; Son, K. N.; Lee, S. J.; Kang, T. I.; Han, M. S.; Jeon, S. J. *Tetrahedron Lett.* **1998**, 39, 3167-3170.

(38) Chou, S.-S.; Hsu, G.-T.; Lin, H.-C. *Tetrahedron Lett.* **1999**, 40, 2157-2160.

(39) Illien, B.; Jehan, P.; Botrel, A.; Darchen, A.; Ledoux-Rak, I.; Zyss, J.; Lahcene, O. *New J. Chem.* **1998**, 22, 633-641.

(40) Jen, A. K.-Y.; Rao, V. P.; Wong, K. Y.; Drost, K. J. *J. Chem. Soc., Chem. Commun.* **1993**, 90-92.

(41) Rao, V. P.; Jen, A. K.-Y.; Wong, K. Y.; Drost, K. J. *Tetrahedron Lett.* **1993**, 34, 1747-1750.

(42) Rao, V. P.; Jen, A. K.-Y.; Chandrasekhar, J.; Namboothiri, I. N. N.; Rathna, A. *J. Am. Chem. Soc.* **1996**, 118, 12443-12448.

(43) Wong, K. Y.; Jen, A. K.-Y.; Rao, V. P.; Drost, K. J. *J. Chem. Phys.* **1994**, 100, 6818-6825.

(44) Ma, H.; Liu, S.; Luo, J.; Suresh, S.; Liu, L.; Kang, S. H.; Haller, M.; Sassa, T.; Dalton, L. R.; Jen, A. K.-Y. *Adv. Funct. Mater.* **2002**, 12, 565-574.

Chapter 3 – Synthesis and Characterization of Chromophores with Novel Donors

Section 1: Previous Donor Research

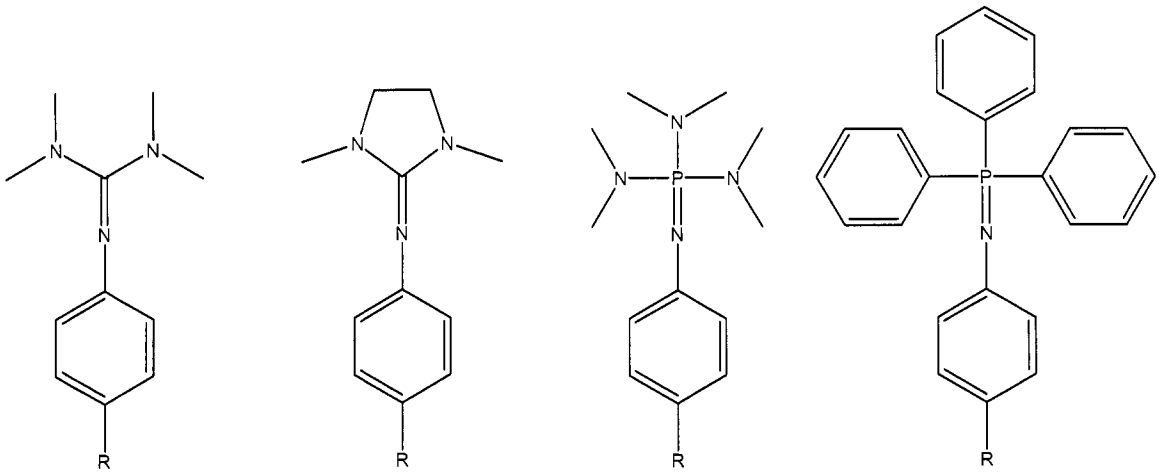

Figure 3.1 Examples of imine donors in literature

Literature is replete with articles detailing research devoted to modification of bridges and acceptors, but the relatively small number of articles published on the subject of donors suggests that they have been largely neglected. Systems based on oxygen and sulfur have been explored, but the former proved to perform poorly while the latter suffers from stability problems.[1] The standard dialkyl and diaryl amino donor systems have been successful, but evidence in the literature suggests that superior systems exist.[2,3] These unconventional guanidine and phosphorous based donor systems demonstrate

significantly enhanced $\mu\beta$ values in small chromophores in conjunction with high degrees of thermal stability. Literature suggests that integration of these imino donors into modern chromophore molecules should yield significant improvements to β resulting in increased r_{33} values and enhanced device performance without sacrificing stability or transparency.[2,3]

Section 2: Proposed Investigation of Donor Systems

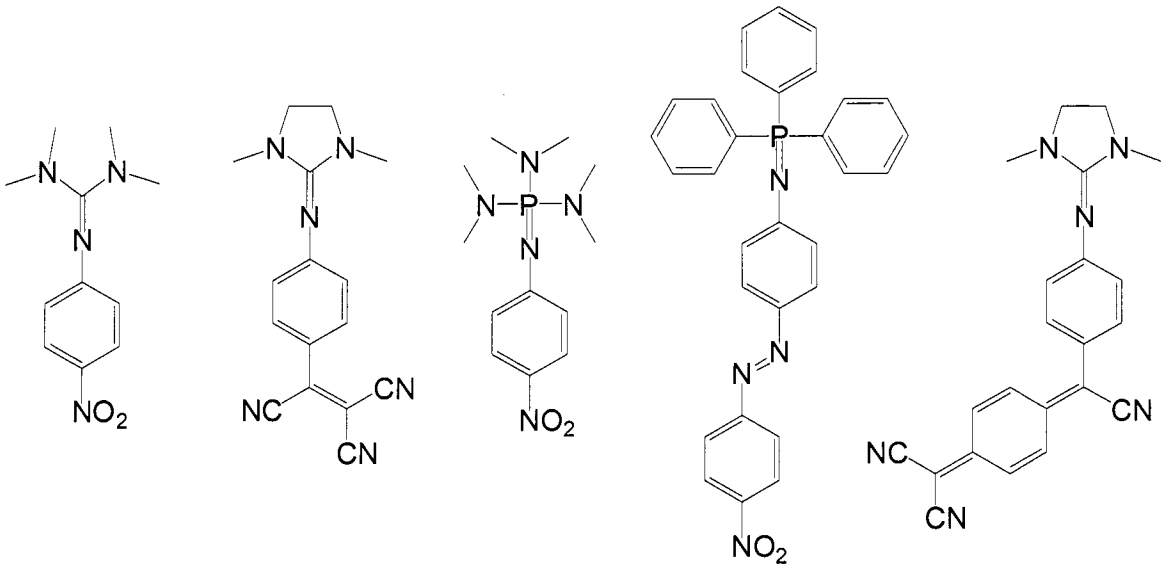

Figure 3.2 Previously synthesized chromophores with imine donors

The enhanced $\mu\beta$ values, good transparency properties, and high thermal stabilities reported in the literature motivated the decision to further explore these novel donor structures. Reported chromophores consisted only of simple donor-acceptor

designs, lacking good bridge systems or advanced acceptors.[2,3] Of the previously explored donors, the aminophosphorane appeared to offer the highest degree of compatibility with integration into modern chromophores. The reported preparation for chromophores containing the aminophosphorane donor involved nucleophilic substitution of *p*-fluoronitrobenzene under mild conditions.[2] Attempts at duplicating these results using *p*-fluorobenzaldehyde or fluorobenzene substituted with the TCF acceptor failed. These attempts are illustrated in Figure 3.3.

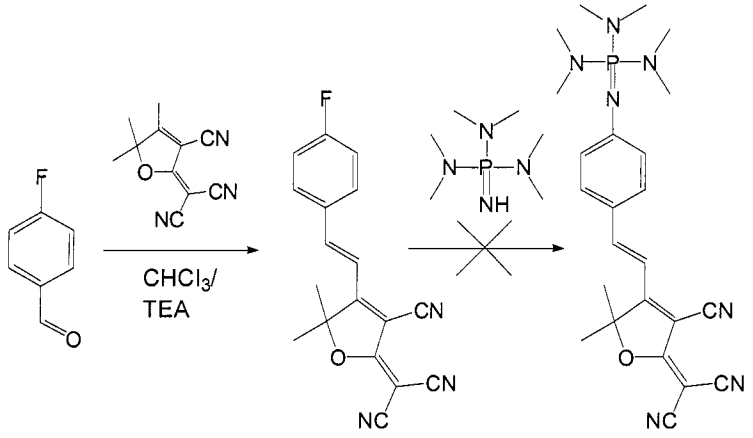

Figure 3.3 Attempted synthesis of aminophosporane donor chromophore

Difficulties in synthesizing chromophores containing the aminophosphorane donor spurred efforts to generate chromophores containing guanidine donors. The generation of chromophores containing guanidine donors appeared to be a rather straightforward operation. In the literature, chromophores containing this donor were synthesized by reaction of anilines with 1,3-dimethyl-2-imidazolidinone or

tetramethylurea in the presence of $POCl_3$.[3] Figure 3.4 illustrates a scheme proposed to integrate guanidine donors into modern chromophores.

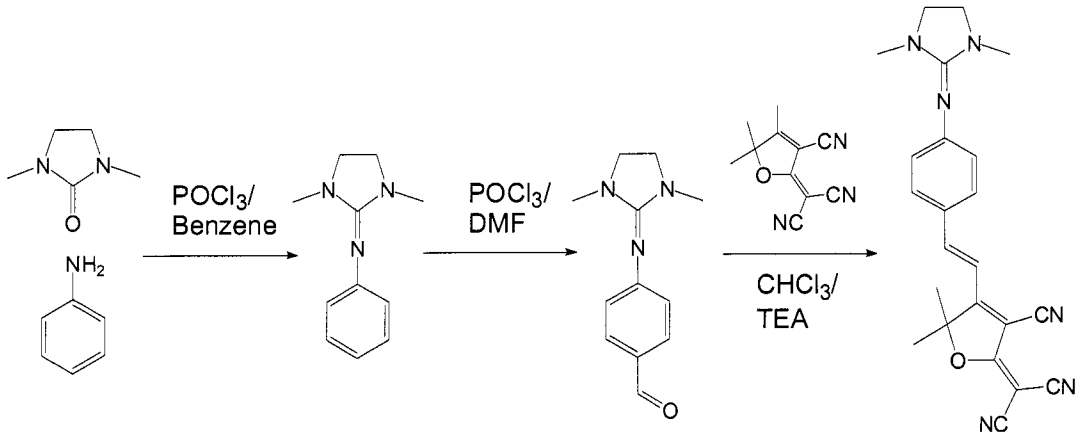

Figure 3.4 Proposed scheme for guanidine donor integration

The proposed scheme ran into problems involving generation of the aldehyde for condensation with the acceptor. As depicted in Figure 3.5, many attempts were made to formylate, but each of them returned starting material. After several repetitions were made for each set of conditions, it became apparent that a new route was needed. Attempts were made to generate the *p*-bromo material in hopes that the halide would facilitate BuLi/DMF formylation or allow Heck coupling reaction. The conditions used to generate the guanidine donor resulted in polymerization of the *p*-bromoaniline. A new and mild preparation of guanidine donors was required.

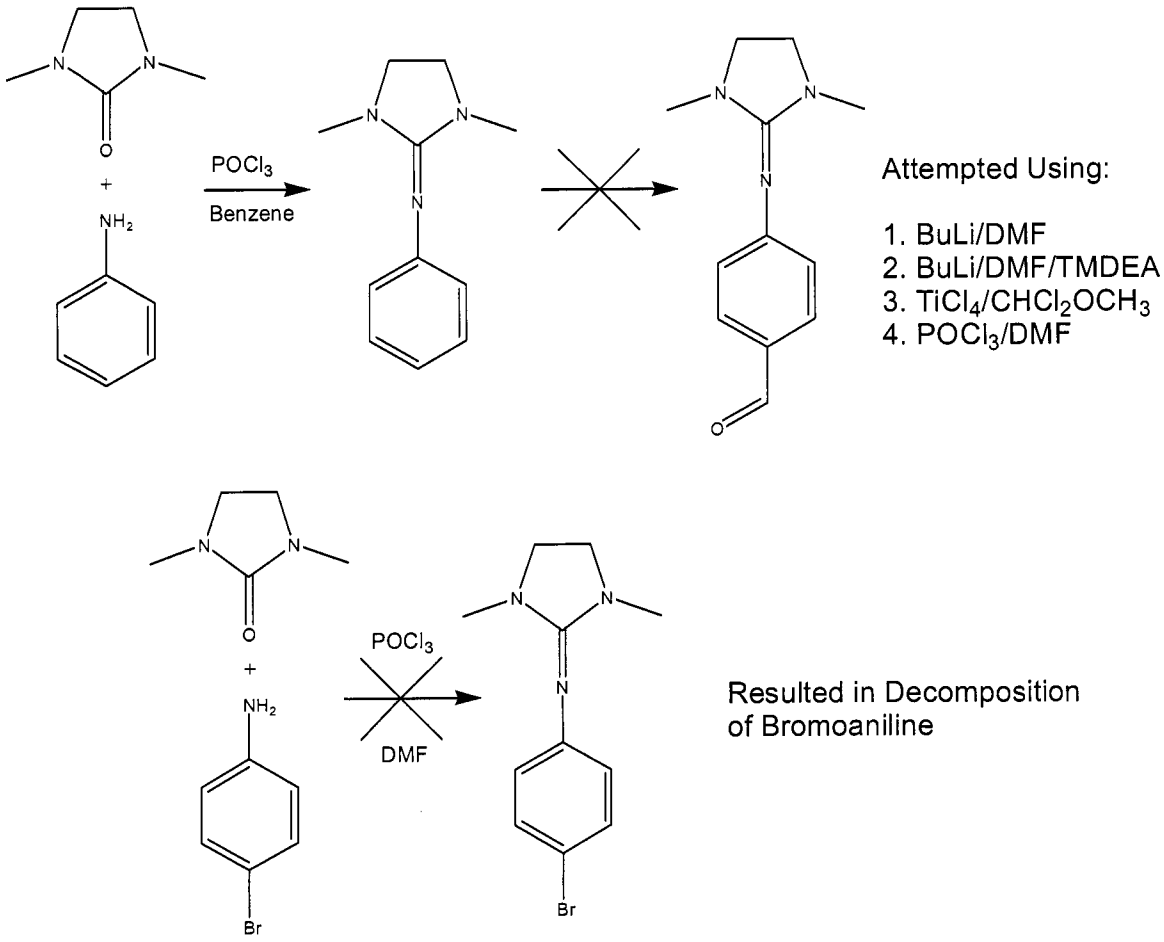

Figure 3.5 Attempts at using literature preparation to generate donor aldehyde

Section 3: Revised Synthesis of Guanidine Donors

A very mild and efficient method for preparing guanidine-based donors from primary arylamines and imidazolium chlorides was found.[4] The use of imidazolium chlorides allowed access to various guanidine-containing materials, but it soon become apparent that these substances were incompatible with conventional column chromatography techniques. Guanidine-containing structures demonstrated a high affinity for both alumina and silica gel presumably due to protonation. Guanidines were first explored as donors due to their extreme ease of protonation hinting at their capacity as donors in NLO systems.[3] All attempts at running guanidines on silica and alumina columns failed despite the addition of triethylamine to the mobile phase in attempts to mitigate protonation. It was decided that the guanidine-donor must be generated at the last step to minimize purification difficulties. Preparation of guanidine-containing chromophores using this methodology requires generation of primary arylamines, yet primary amines are incompatible with common chromophore synthetic chemistry. Thus the necessary materials were synthesized from nitro analogs. A selective and mild nitro reduction was found that left vinylic and cyano moieties intact. Figure 3.6 depicts synthesis of a simple chromophore using this scheme.[5]

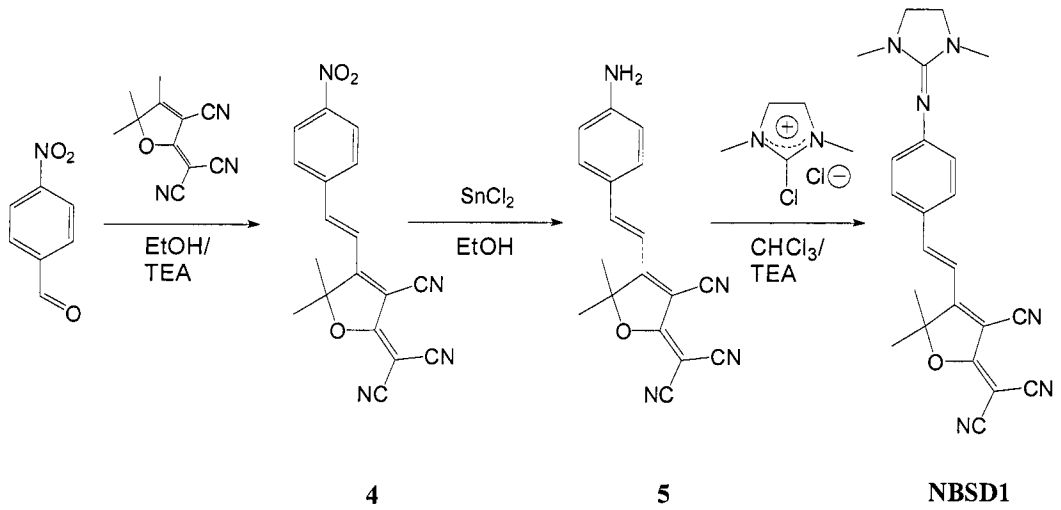

Figure 3.6 Synthesis of a small chromophore by reduction of nitro analog and reaction with imidazolium chloride

The TCF-1 chromophore, containing a conventional amino donor, was selected as a reference compound for comparison to the NBSD1 chromophore and its guanidine donor. The stable, synthetically accessible and efficient FTC skeleton was chosen as the base structure for the next family of chromophores to be synthesized. During synthesis of the NBSD1 chromophore, it was noted that compound **4** possessed limited solubility. The decision was made to use a 3,4-dibutyl-thiophene bridge to prevent possible synthetic and purification issues related to insolubility of the nitro intermediates. Conventional chromophore chemistry was used by Lafe Purvis to synthesize the NBLP reference compound.

The synthetic scheme used to prepare NBSD1 was adapted to a relatively standard FTC synthesis. A nitro-containing analog of the desired chromophore was synthesized by a similar route conventional chromophore syntheses. Synthesis of the nitro materials proceeded without issue and these materials demonstrated good stability and compatibility with conventional chromophore chemistry. This nitro analog was then reduced under similar conditions to those used for the NBSD1 synthesis, and the resulting amine was reacted with the imidazolium chloride salt to yield the desired chromophore as shown in Figure 3.7.

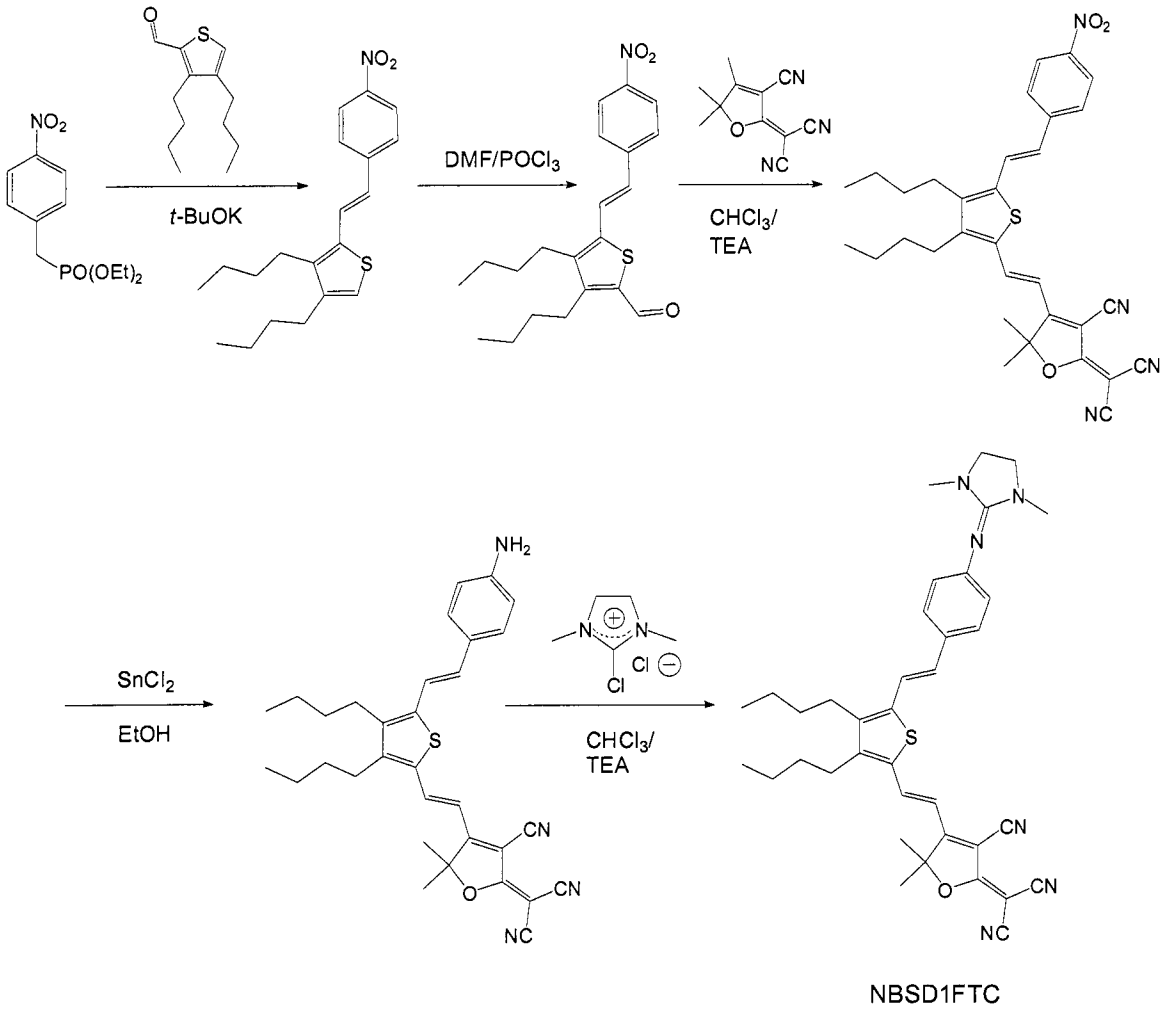

Figure 3.7 Revised synthetic scheme for chromophores with guanidine donors

As previously discussed, the response of NLO chromophores to an applied electric field may be approximated as a reversible charge transfer from the donor to the acceptor moiety. This simplified model may be used to conceptualize the behavior of high β chromophores and guide design. Chromophores with large NLO susceptibilities generally have a very red-shifted λ_{max} suggesting a small HOMO-LUMO gap.[6] This

knowledge may be used to design systems with increased β value by lowering the energy of the charge transfer state. Guanidine-based donors appeared to provide a good template on which to build systems with stabilized charge transfer states. Figure 3.8 depicts a benzo-guanidine derivative of the guanidine system in which the donor should possess some degree of aromatic stabilization in the charge transfer state.

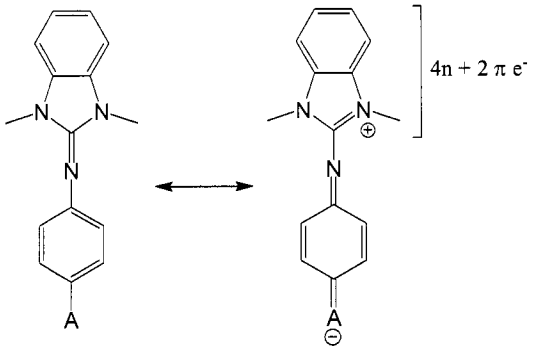

Figure 3.8 Aromatic stabilization of the charge-separated resonance structure

The benzimidazolium chloride salt needed to generate benzo-guanidine chromophores was synthesized from 2-hydroxybenzimidazole. This material was dimethylated with sodium hydride and methyl iodide. The dimethylated material was converted to the benzimidazolium chloride salt through adaptation of literature procedure.[5] Formation proceeded in lower yield than the imidazolium chloride, presumably due to the increased solubility of the benzimidazolium chloride. Reaction of the salt with the amino precursor to produce the NBSD2FTC chromophore proceeded efficiently.

Section 4: Results and Discussion

Table 3.1 Data for NBLP, NBSD1FTC and NBSD2FTC chromophores

Chromophore	λ_{max} $CHCl_3$ (nm)	β_{HRS} / β_{CHCl3}*	r_{33} in pm/V**	T_D (DSC) in °C
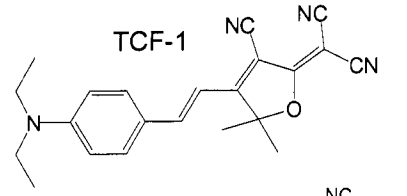 TCF-1	584	1993 ± 62	--	--
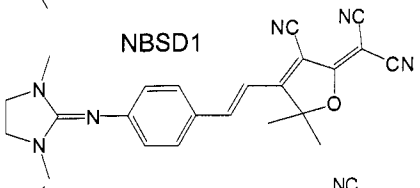 NBSD1	560	2501 ± 87	--	--
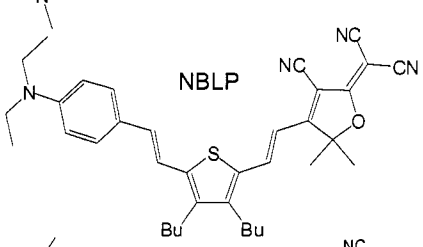 NBLP	700	10769 ± 664	40	220
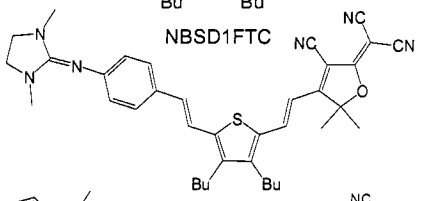 NBSD1FTC	642	5138 ± 687	15	310
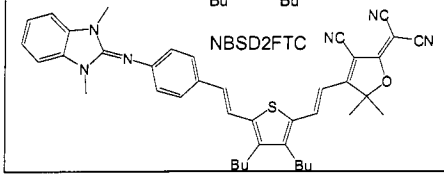 NBSD2FTC	650	6182 ± 477	17	250

*measured in chloroform at 880 nm

**20% by weight in APC measured at 1300 nm by simple reflection technique

The NBSD1 chromophore displays the highly desirable and unusual properties of a significantly improved β value at 880 nm with a λ_{max} in $CHCl_3$ shifted 24 nm away from telecommunication wavelengths when compared to the conventional donor system. Chromophores with larger β values generally demonstrate a red-shifted λ_{max} which can lead to significant absorption problems in devices.[1,7,8] The extremely desirable combination of increased β in conjunction with a blue-shifted λ_{max} displayed by the NBSD1 chromophore in these preliminary result encouraged efforts to synthesize more complex NBSD1FTC and NBSD2FTC chromophores.

Similar to the NBSD1 and TCF-1 chromophores, the guanidine-containing FTC chromophores were blue-shifted relative to the NBLP chromophore. This shift was more pronounced with the NBSD1FTC and NBSD2FTC chromophores being blue-shifted 58 and 50 nm respectively. Unlike the smaller chromophores, the guanidine-containing FTC chromophores displayed significantly lower β values than the NBLP chromophore at 880 nm. The NBSD2FTC chromophore displayed a slightly red-shifted λ_{max} and somewhat larger β value than the NBSD1FTC chromophore possibly due to aromatic stabilization of the charge transfer state. In line with the β values, NBSD2FTC displayed a slightly larger r_{33} than NBSD1FTC, but both with considerably lower values than the NBLP chromophore.

Clearly the results for the NBSD1FTC and NBSD2FTC chromophores do not correlate with the performance of the smaller NBSD1 chromophore. Both the smaller NBSD1 and the guanidine-containing FTC chromophores demonstrate a blue shifted λ_{max}, but the NBSD1 chromophore has an enhanced β value while the NBSD1FTC and NBSD2FTC molecules have inferior β values when compared to reference compounds. It is possible that resonance enhancement is responsible for the observed behavior. The λ_{max} of the NBSD1 chromophore is closer to 2ω resonance at 880 nm than that of the TCF-1 chromophore. Conversely, the λ_{max} of the NBLP chromophore is closer to ω resonance at 880 nm that those of the NBSD1FTC and NBSD2FTC chromophores. Despite the fact that β measurements are resonance dependent, the r_{33} data reflects a similar trend despite being measured at a 1300 nm. A more plausible explanation for this unexpected behavior is related to the structure of the guanidine donors.

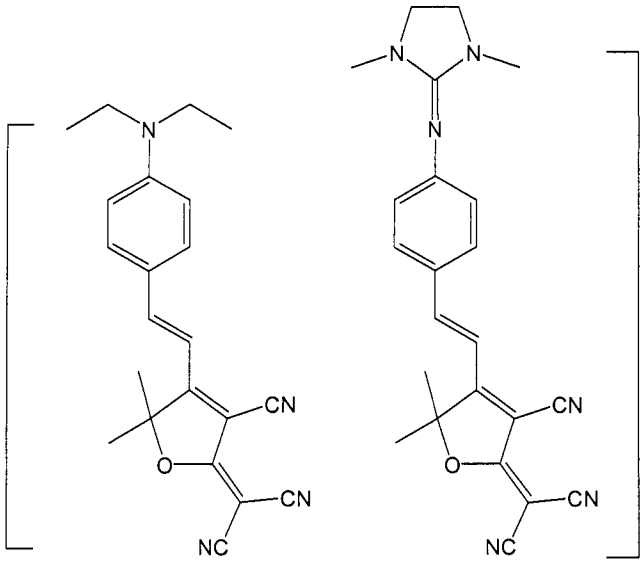

TCF-1 NBSD1

Figure 3.9 Conjugation length of TCF-1 and NBSD1 chromophores

Increasing the length of conjugation between the donor and acceptor in NLO chromophores generally results in an improved β value. These guanidine-based donors possess modestly-increased conjugation length compared to simple amino donors. If guanidine-based donors are weaker than amino donors, it possible that the increased conjugation length of guanidine-containing donors offsets the decreased donor potency, resulting in an overall enhancement of β in short chromophores. In chromophore with lengthy conjugation between the donor and acceptor, the increased conjugation length of the guanidine donor is less significant and presumably would have a less pronounced effect. It is likely that the enhancement of β from slightly increased conjugation length

would not be able to overcome the decrease in β due to the reduction in donor strength in longer chromophores.

Despite the decreased β values observed for larger chromophores, guanidine-based acceptors offer promising characteristics. The thermal stabilities observed for guanidine containing chromophores are significantly higher than those offered by similar amino systems. Guanidine-based donors could be valuable for thermally demanding applications. These donors are ideally suited to short chromophores where they can simultaneously offer superior thermal stability, transparency and NLO characteristics compared to amino materials.

Section 5: Conclusions

Although guanidine donors show potential for a fairly limited range of applications, the results of this study strongly suggest that they are generally inferior to amino donors while explaining the data reported in the literature.[2,3] The information gained from this donor study not only provides some qualitative insight into the relationship between donor/acceptor and conjugation, but will serve as a useful tool for interpreting the results of future donor research. With these perplexing results explained and the superiority of amino donors once again established, efforts may be focused upon bridge and acceptor modification.

Section 6: Experimental Section

All commercially available starting materials were purchased from Aldrich or ACROS and used without further purification unless otherwise noted. HPLC grade tetrahydrofuran and diethyl ether were purchased from Fisher chemical and distilled from sodium and benzophenone immediately before use. HPLC grade methylene chloride was also purchase from Fisher and distilled from CaH prior to use. Reagent grade triethylamine was purchased from Aldrich and distilled from CaH. All reactions performed under nitrogen unless otherwise stated. Alkyl lithium reagents were purchased from ACROS and titrated using 4-biphenylmethanol according to literature procedure.[9] The imidazolium chlorides, compounds **1** and **3**, were prepared from literature procedure.[4] The resulting crystals are extremely hygroscopic and should handled under moisture-free conditions.

Absorption spectra of chromophore solutions obtained in chloroform with trace triethylamine to inhibit protonation using a Shimadzu 1601 UV-Vis spectrophotometer at 250-1000 nm. Decomposition temperature measured using a Shimadzu DSC-60 differential scanning calorimeter (DSC) under nitrogen flow at a temperature ramp rate of 5°C per minute. NMR spectra were obtained using a 300 MHz Bruker Avance NMR spectrometer in deuterated chloroform or DMSO purchased from Cambridge Isotope

Laboratories Inc. Low-resolution mass spectral data was collected on a PerSeptive Biosystems Mariner ESI-TOF spectrometer. High-resolution mass analysis was performed on a Thermo-electron Carburation Finnigan LTQ-FT mass specrometer. 200 nM to 4 uM solutions of chromophore in chloroform containing trace triethylamine to inhibit protonation were used to obtain HRS data. Details of the femtosecond HRS experiment may be found elsewhere.[10] All HRS measurement were performed by Kim Firestone and David Lao. Measurements of β are reported relative to β_{CHCl3} as the hyperpolarizability of chloroform is in debate.[10-13] EO films containing 20% by weight active chromophore in amorphous polycarbonate were spin coated onto glass/ITO slides and a gold electrode was sputtered on top of the film. Films were prepared from filtered solutions of 12% solid by weight in distilled cyclopentanone. These films were characterized by Marnie Haller using the simple reflection technique reported by Teng and Man.[14]

The NBSD1FTC and NBSD2FTC chromophores displayed unexpected interactions with solvents. Attempts to recrystallize these chromophores from various solvents resulted in retention of these solvents in the chromophore matrix. Attempts were made to dry the NBSD1FTC chromophore, which contained n-hexane from recrystallization. The chromophore was heated to 50° C under high vacuum for one week, but the mass remained unchanged and NMR confirmed no change in the amount of trapped hexane though no decomposition was visible in the spectra. Cyclohexane was

selected as a final recrystallization solvent because its ^{1}H NMR spectra is simple, making identification and integration easy. The NBSD1FTC and NBSD2FTC chromophores were determined by NMR data to contain 5% and 2% cyclohexane by mass after recrystallization respectively. Preparation of HRS and EO samples were adjusted to account for the presence of solvent. Due to this solvent retention, elemental analysis was not obtained.

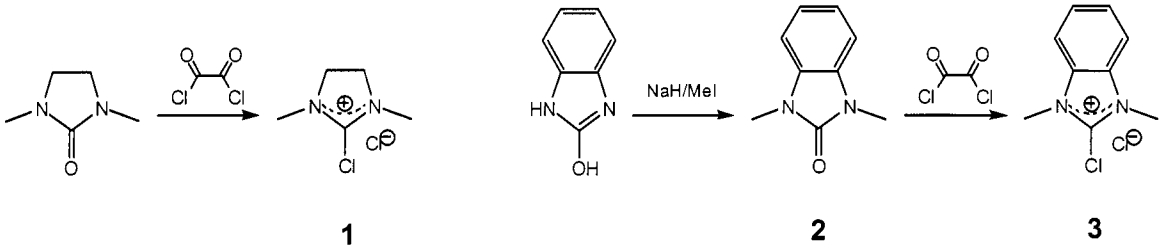

Figure 3.10 Preparation of Imidazolium Chlorides

1,3-dimethyl-2-benzimidazolidinone (2)

5.00g (37.3 mmol) of 2-hydroxybenzimidazole were dissolved in 75 ml of dry THF and 1.97g (82.0 mmol) of sodium hydride was added in portions to the solution. The solution was stirred for 1 hour and then 11.6g (82.0 mmol) of methyl iodide were added dropwise to the solution. The reaction mixture was refluxed overnight and then the THF was removed via rotary evaporation. The residue was extracted with methylene chloride and water. The organic phase was separated, dried with sodium sulfate and the methylene

chloride was removed via rotary evaporation. The residue was loaded onto a silica gel column and was eluted with 60/40 hexane/ethylacetate to yield 5.26g (87%) of faint pink crystals. ^{1}H ($CDCl_3$) δ 7.11 (q, 2H, J = 2.7 Hz), 6.98 (d, 2H, J = 2.7 Hz), 7.71 (s, 6H).

2-{3-Cyano-5,5-dimethyl-4-[2-(4-nitro-phenyl)-vinyl]-5H-furan-2-ylidene}-malononitrile (4)

1.00g (6.62mmol) of 4-nitro-benzaldehyde and 1.98g (9.93 mmol) of 2-(3-Cyano-4,5,5-trimethyl-5H-furan-2-ylidene)-malononitrile were dissolved in 10 ml of chloroform with 10 drops of triethyl amine and the solution was refluxed overnight. The chloroform was removed via rotary evaporation and the residue was purified by silica gel chromatography eluted with methylene chloride to yield 1.63g (74%) of an orange solid. ^{1}H ($CDCl_3$) δ 8.36 (d, 2H, J = 8.7 Hz), 7.83 (d, 2H, J = 8.4 Hz), 7.71 (d, 1H, J = 16.5 Hz), 7.14 (d, 1H, J = 16.5 Hz), 1.85 (s, 6H).

2-{4-[2-(4-Amino-phenyl)-vinyl]-3-cyano-5,5-dimethyl-5H-furan-2-ylidene}-malononitrile (5)

Reduction of the nitro group was accomplished though alteration of literature procedure.[5] 1.00g (3.00 mmol) of 2-{3-Cyano-5,5-dimethyl-4-[2-(4-nitro-phenyl)-vinyl]-5H-furan-2-ylidene}-malononitrile was dissolved in 50 ml of ethanol with 3.40g (15.0 mmol) of stannous chloride dihydrate. The mixture was refluxed overnight and the ethanol removed via rotary evaporation. The residue was purified using silica gel

chromatography eluted with 99/1 methylene chloride/triethylamine to yield 0.834g (92%) of a red solid. ^{1}H (DMSO-d_6) δ 7.88 (d, 1H, J = 15.6 Hz), 7.67 (d, 2H, J = 8.7 Hz), 6.82 (d, 1H, J = 15.6 Hz), 6.66 (d, 2H, J = 8.7 Hz), 5.75 (s, 2H), 1.74 (s, 6H).

2-(3-Cyano-4-{2-[4-(1,3-dimethyl-imidazolidin-2-ylideneamino)-phenyl]-vinyl}-5,5-dimethyl-5H-furan-2-ylidene)-malononitrile (NBSD1)

0.500g (1.65 mmol) of 2-{4-[2-(4-Amino-phenyl)-vinyl]-3-cyano-5,5-dimethyl-5H-furan-2-ylidene}-malononitrile and 0.367g (3.63 mmol) of dry triethylamine were dissolved in 35 ml of dry methylene chloride. 0.307g (1.82 mmol) of 2-chloro-1,3-dimethyl-4,5-dihydro-3H-imidazolium chloride were added to the solution and the reaction was stirred for 2 hours at room temperature and 30 minutes at reflux. The reaction was worked up with sodium bicarbonate solution and the organic phase was dried with sodium sulfate. The methylene chloride was removed via rotary evaporation and the residue was recrystallized from methylene chloride/cyclohexane to yield 0.173g (73%) of a red solid. ^{1}H (DMSO-d_6) δ 7.91 (d, 1H, J = 15.9 Hz), 7.71 (d, 2H, J = 8.7 Hz), 6.91 (d, 1H, J = 15.9 Hz), 6.74 (d, 2H, J = 8.7 Hz), 3.45 (s, 4H), 2.65 (s, 6H), 1.76 (s, 6H). MS *m/z* calcd 399.2; found 399.2.

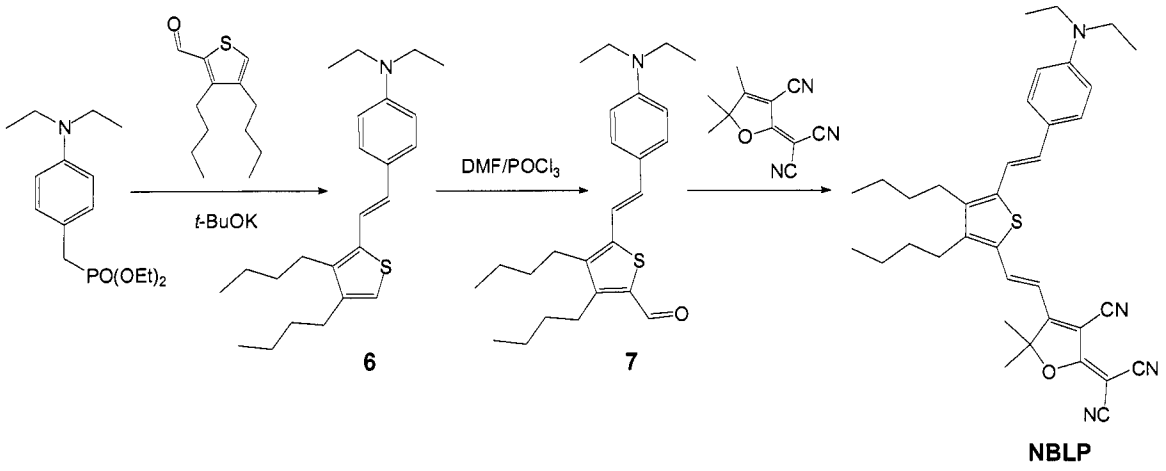

Figure 3.11 Synthetic Scheme for NBLP reference compound

{4-[2-(3,4-Dibutyl-thiophen-2-yl)-vinyl]-phenyl}-diethyl-amine (6)

5.48g (18.3 mmol) of (4-Diethylamino-benzyl)-diethyl-phosphonate and 3.70g (16.5 mmol) 3,4-Dibutyl-thiophene-2-carbaldehyde were dissolved in dry 70 ml of THF under nitrogen and the solution was cooled to 0° C. 18.3ml of 1M *t*-BuOK in THF were added dropwise to the solution and the solution was stirred at 0° C for 1 hour. The solution was allowed to warm to room temperature and was stirred for an additional hour before being quenched with water. The THF was removed via rotary evaporation and the residue was extracted with methylene chloride and water. The organic phase was saved and dried with sodium sulfate and removed via rotary evaporation. Methylene chloride was used to elute the residue through a silica gel plug to yield 5.31g (87%) of an orange solid. ^{1}H ($CDCl_3$) δ 7.34 (d, 2H, J = 8.7 Hz), 7.03 (d, 1H, J = 15.9 Hz), 6.81 (d, 1H, J = 15.9 Hz),

6.68 (d, 2H, J = 8.7 Hz), 6.65 (s, 1H), 3.38 (q, 4H, J = 6.9 Hz), 2.62 (t, 2H, J = 7.2 Hz), 2.50 (t, 2H, J = 7.5 Hz), 1.44 (m, 8H), 1.11 (t, 6H, J = 6.9 Hz), 0.93 (t, 6H, J = 7.2 Hz).

3,4-Dibutyl-5-[2-(4-diethylamino-phenyl)-vinyl]-thiophene-2-carbaldehyde (7)

3.12g (8.44 mmol) of {4-[2-(3,4-Dibutyl-thiophen-2-yl)-vinyl]-phenyl}-diethyl-amine were dissolved into 75 ml of dry 1,2-dichloroethane at room temperature. To this solution 0.648 g (8.86 mmol) of dry DMF and 1.36g (8.86 mmol) of $POCl_3$ were added successively. Solution was refluxed overnight and quenched with 2M sodium acetate solution. The mixture was stirred for 2 hours and then extracted with methylene chloride. The methylene chloride was dried with sodium sulfate and removed via rotary evaporation and the residue was purified via silica gel chromatography eluted with 20/80 ethylacetate/hexane to yield 2.45g (73%) of a red solid. ^{1}H (DMSO-d_6) δ 9.95 (s, 1H), 7.47 (d, 2H, J = 8.7 Hz), 7.13 (d, 1H, J = 15.9 Hz), 7.04 (d, 1H, J = 15.9 Hz), 6.67 (d, 2H, J = 9.0 Hz), 3.38 (q, 4H, J = 6.9 Hz), 2.90 (m, 4H), 1.42 (m, 8H), 1.11 (t, 6H, J = 6.9 Hz), 0.93 (m, 6H).

2-[3-Cyano-4-(2-{3,4-dibutyl-5-[2-(4-diethylamino-phenyl)-vinyl]-thiophen-2-yl}-vinyl)-5,5-dimethyl-5H-furan-2-ylidene]-malononitrile (NBLP)

1.00 g (2.51 mmol) of 3,4-Dibutyl-5-[2-(4-diethylamino-phenyl)-vinyl]-thiophene-2-carbaldehyde and 0.600 g (3.01 mmol) of 2-(3-Cyano-4,5,5-trimethyl-5H-furan-2-

ylidene)-malononitrile were dissolved in 8.0 ml of chloroform with 3 drops of triethyl amine and the solution was refluxed overnight. The chloroform was removed via rotary evaporation and the residue was purified by silica gel chromatography eluted with methylene chloride. Material was recrystallized methylene chloride/cyclohexane to yield 1.03g (71%) of a green solid. ^{1}H (DMSO-d_6) δ 8.16 (d, 1H, J = 15.3 Hz), 7.51 (d, 2H, J = 9.0 Hz), 7.21 (d, 1H, J = 15.6 Hz), 7.11 (d, 1H, J = 15.6 Hz), 6.69 (d, 2H, J = 9.0 Hz), 6.59 (d, 1H, J = 15.0 Hz), 3.44 (q, 4H, J = 6.9 Hz), 2.72 (m, 4H), 1.72 (s, 6H), 1.43 (m, 8H), 1.12 (t, 6H, J = 6.9 Hz), 0.92 (m, 6H). MS *m/z* calcd 579.3152; found 579.3102.

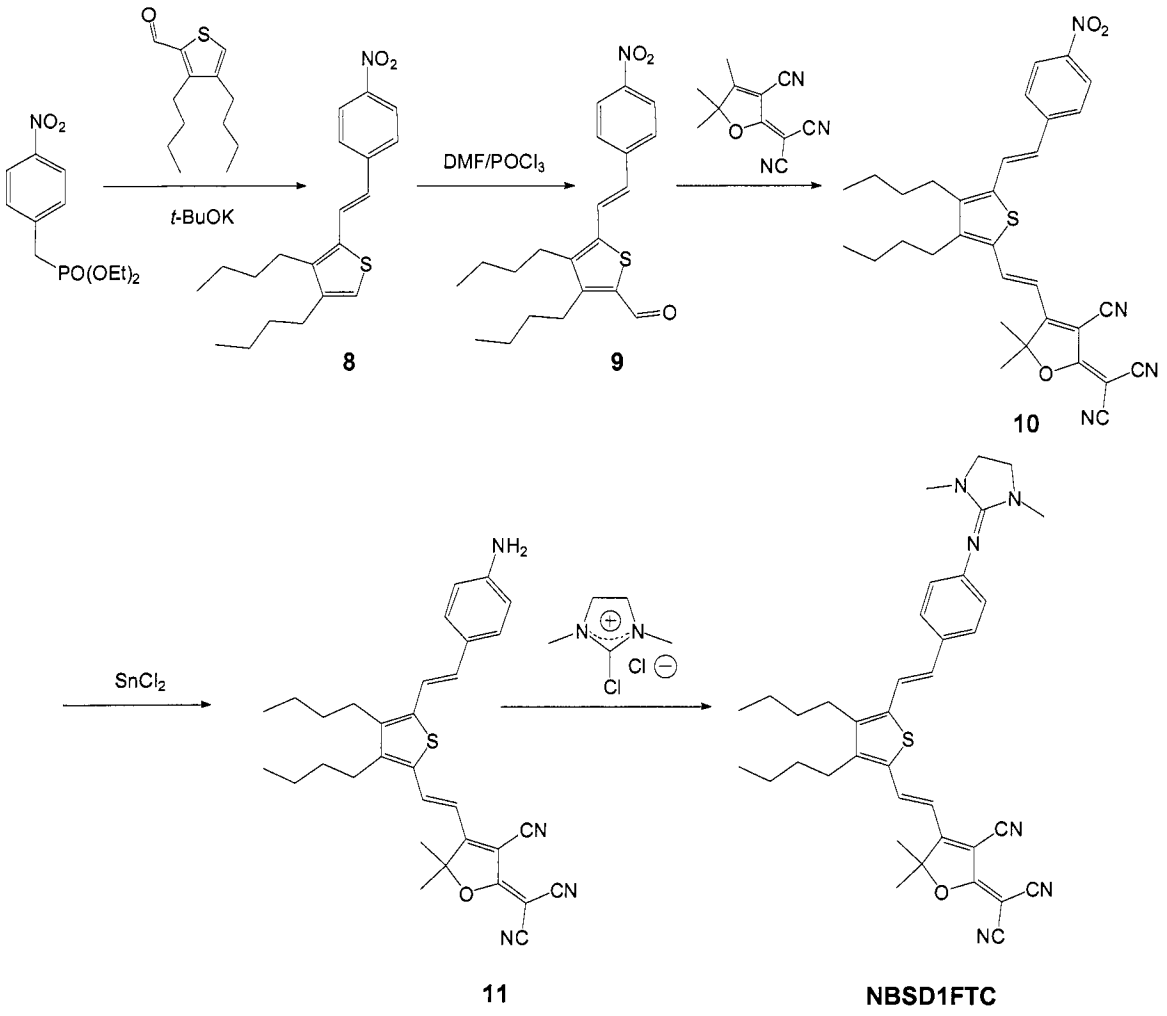

Figure 3.12 Synthetic scheme used for NBSD1FTC and NBSD2FTC chromophores

3,4-Dibutyl-2-[2-(4-nitro-phenyl)-vinyl]-thiophene (8)

5.00g (18.3mmol) of (4-nitro-benzyl)-diethyl-phosphonate and 3.70g (16.5mmol) 3,4-Dibutyl-thiophene-2-carbaldehyde were dissolved in dry 70 ml of THF under nitrogen and the solution was cooled to 0° C. 18.3ml of 1M *t*-BuOK in THF were added dropwise to the solution and the solution was stirred at 0° C for 1 hour. The solution was allowed

to warm to room temperature and was stirred for an additional hour before being quenched with water. The THF was removed via rotary evaporation and the residue was extracted with methylene chloride and water. The organic phase was saved and dried with sodium sulfate and removed via rotary evaporation. Methylene chloride was used to elute the residue through a silica gel plug to yield 5.08g (90%) of an orange solid. ^{1}H (DMSO-d_6) δ 8.20 (d, 2H, J = 6.9 Hz), 7.89 (d, 2H, J = 7.2 Hz), 7.69 (d, 1H, J = 15.6 Hz), 7.17 (s, 1H), 6.98 (d, 1H, J = 15.9 Hz), 2.73 (t, 4H, J = 7.1 Hz), 1.50 (m, 8H), 0.93 (t, 6H J = 6.3 Hz).

3,4-Dibutyl-5-[2-(4-nitro-phenyl)-vinyl]-thiophene-2-carboxaldehyde (9)

2.90g (8.44mmol) of 3,4-dibutyl-2-[2-(4-nitro-phenyl)-vinyl]-thiophene were dissolved into 75 ml of dry 1,2-dichloroethane at room temperature. To this solution 0.648 g (8.86 mmol) of dry DMF and 1.36g (8.86 mmol) of $POCl_3$ were added successively. Solution was refluxed overnight and quenched with 2M sodium acetate solution. The mixture was stirred for 2 hours and then extracted with methylene chloride. The methylene chloride was dried with sodium sulfate and removed via rotary evaporation and the residue was purified via silica gel chromatography eluted with 20/80 ethylacetate/hexane to yield 2.71g (86%) of an orange solid. ^{1}H (DMSO-d_6) δ 10.03 (s, 1H), 8.24 (d, 2H, J = 9.0 Hz), 7.99 (d, 2H, J = 9.0 Hz), 7.75 (d, 1H, J = 16.2 Hz), 7.33 (d, 1H, J = 16.2 Hz), 2.77 (m, 4H), 1.50 (m, 8H), 0.92 (t, 6H J = 6.0 Hz).

2-[3-Cyano-4-(2-{3,4-dibutyl-5-[2-(4-nitro-phenyl)-vinyl]-thiophen-2-yl}-vinyl)-5,5-dimethyl-5H-furan-2-ylidene]-malononitrile (10)

1.00g (2.69mmol) of 3,4-dibutyl-5-[2-(4-nitro-phenyl)-vinyl]-thiophene-2-carboxaldehyde and 0.643g (3.23 mmol) of 2-(3-Cyano-4,5,5-trimethyl-5H-furan-2-ylidene)-malononitrile were dissolved in 8.0 ml of chloroform with 3 drops of triethyl amine and the solution was refluxed overnight. The chloroform was removed via rotary evaporation and the residue was purified by silica gel chromatography eluted with methylene chloride to yield 1.30g (87%) of a green solid. ^{1}H (DMSO-d_6) δ 8.24 (d, 2H, J = 9.0 Hz), 8.13 (d, 1H, J = 15.6 Hz), 7.99 (d, 2H, J = 9.0 Hz), 7.79 (d, 1H, J = 15.9 Hz), 7.31 (d, 1H, J = 15.9 Hz), 6.76 (d, 1H, J = 15.6 Hz), 2.80 (m, 4H), 1.76 (s, 6H), 1.43 (m, 8H), 0.93 (t, 6H J = 5.7 Hz).

2-[4-(2-{5-[2-(4-Amino-phenyl)-vinyl]-3,4-dibutyl-thiophen-2-yl}-vinyl)-3-cyano-5,5-dimethyl-5H-furan-2-ylidene]-malononitrile (11)

Reduction of the nitro group was accomplished though alteration of literature procedure.[5] 1.00g (1.81 mmol) of 2-[3-cyano-4-(2-{3,4-dibutyl-5-[2-(4-nitro-phenyl)-vinyl]-thiophen-2-yl}-vinyl)-5,5-dimethyl-5H-furan-2-ylidene]-malononitrile was dissolved in 25 ml of ethanol with 2.04g (9.00 mmol) of stannous chloride dihydrate. The mixture was refluxed overnight and the ethanol removed via rotary evaporation. The residue was purified using silica gel chromatography eluted with 99/1 methylene chloride/triethylamine to yield 0.490g (52%) of a green solid. ^{1}H (DMSO-d_6) δ 8.18 (d,

1H, J = 15.6 Hz), 7.40 (d, 2H, J =8.7 Hz), 7.19 (d, 1H, J = 15.9 Hz), 7.07 (d, 1H, J = 15.9 Hz), 6.60 (m, 3H), 5.72 (s, 2H), 2.72 (m, 4H), 1.73 (s, 6H), 1.43 (m, 8H), 0.93 (m, 6H).

2-{3-Cyano-4-[2-(3,4-dibutyl-5-{2-[4-(1,3-dimethyl-imidazolidin-2-ylideneamino)-phenyl]-vinyl}-thiophen-2-yl)-vinyl]-5,5-dimethyl-5H-furan-2-ylidene}-malononitrile (NBSD1FTC)

0.200g (0.383 mmol) of 2-[4-(2-{5-[2-(4-amino-phenyl)-vinyl]-3,4-dibutyl-thiophen-2-yl}-vinyl)-3-cyano-5,5-dimethyl-5H-furan-2-ylidene]-malononitrile and 0.0853g (0.843 mmol) of dry triethylamine were dissolved in 20 ml of dry methylene chloride. 0.0712g (0.421 mmol) of 2-chloro-1,3-dimethyl-4,5-dihydro-3H-imidazolium chloride were added to the solution and the reaction was stirred for 2 hours at room temperature and 30 minutes at reflux. The reaction was worked up with sodium bicarbonate solution and the organic phase was dried with sodium sulfate. The methylene chloride was removed via rotary evaporation and the residue was recrystallized from methylene chloride/cyclohexane to yield 0.173g (73%) of a blue solid. ^{1}H (DMSO-d_6) δ 8.21 (d, 1H, J = 15.6 Hz), 7.54 (d, 2H, J = 8.7 Hz), 7.36 (d, 1H, J = 15.9 Hz), 7.17 (d, 1H, J = 15.6 Hz), 6.79 (d, 2H, J = 8.4 Hz), 6.67 (d, 1H, J = 15.3 Hz), 3.36 (s, 4H), 2.74 (m, 4H), 2.63 (s, 6H), 1.77 (s, 6H), 1.40 (m, 8H), 0.95 (m, 6H). MS *m/z* calcd 619.3214; found 619.3240.

2-{3-Cyano-4-[2-(3,4-dibutyl-5-{2-[4-(1,3-dimethyl-1,3-dihydro-benzoimidazol-2-ylideneamino)-phenyl]-vinyl}-thiophen-2-yl)-vinyl]-5,5-dimethyl-5H-furan-2-ylidene}-malononitrile (NBSD2FTC)

0.200g (0.383 mmol) of 2-[4-(2-{5-[2-(4-amino-phenyl)-vinyl]-3,4-dibutyl-thiophen-2-yl}-vinyl)-3-cyano-5,5-dimethyl-5H-furan-2-ylidene]-malononitrile and 0.0853g (0.843 mmol) of dry triethylamine were dissolved in 20 ml of dry methylene chloride. 0.0913g (0.421 mmol) of 2-chloro-1,3-dimethyl-3H-benzoimidazolium chloride were added to the solution and the reaction was stirred for 2 hours at room temperature and 30 minutes at reflux. The reaction was worked up with sodium bicarbonate solution and the organic phase was dried with sodium sulfate. The methylene chloride was removed via rotary evaporation and the residue was recrystallized from methylene chloride/cyclohexane to yield 0.184g (72%) of a blue solid. ^{1}H (DMSO-d_6) δ 8.18 (d, 1H, J = 15.3 Hz), 7.57 (d, 2H, J = 8.4 Hz), 7.35 (d, 1H, J = 15.9 Hz), 7.14 (m, 5H), 6.86 (d, 2H, J = 8.4 Hz), 6.64 (d, 1H, J = 15.3 Hz), 3.25 (s, 6H), 2.75 (m, 4H), 1.74 (s, 6H), 1.43 (m, 8H), 0.92 (m, 6H). MS *m/z* calcd 667.3214; found 667.3147.

Notes to Chapter 3

(1) Dalton, L. R. *Adv. Polym. Sci.* **2002**, 158, 1-68.

(2) Katti, K. V.; Raghuraman, K.; Pillarsetty, N.; Karra, S. R.; Gulotty, R. J.; Chartier, M. A.; Langhoff, C. A. *Chem. Mater.* **2002**, 14, 2436-2438.

(3) Boldt, P.; Eisentrager, T.; Glania, C.; Goldenitz, J.; Kramer, P.; Matschiner, R.; Rase, J.; Schwesinger, R.; Wichern, J.; Wortmann, R. *Adv. Mater.* **1996**, 8, 672-675.

(4) Isobe, T.; Fukuda, K.; Ishikawa, T. *Tetrahedron: Asymmetry*, **1998**, 9, 1729-1735.

(5) Bellamy, F. D.; Ou, K. *Tet. Lett.* **1984**, 25, 839-842.

(6) Oudar, J. L.; Chemla, D. S. *J. Chem. Phys.* **1977**, 66, 2664-2668.

(7) Raimundo, J.-M.; Blanchard, P.; Gallego-Planas, N.; Mercier, N.; Ledoux-Rak, I.; Hierle, R.; Roncali, J. *J. Org. Chem.* **2002**, 67, 205-218.

(8) Rao, V. P.; Wong, K. Y.; Jen, A. K.-Y.; Drost, K. J. *Chem. Mater.* **1994**, 6, 2210-2212.

(9) Kofron, W. G.; Baclawski, L. M. *J. Org. Chem.* **1976**, 41, 1879-1880.

(10) Firestone, K. A.; Reid, P. J.; Lawson, R.; Jang, S.-H.; Dalton, L. R. *Inorg. Chim. Acta.* **2004**, 357, 3957-3966.

(11) Clays, K.; Persoons, A. *Phys. Rev. Lett.* **1991**, 66, 2980-2983.

(12) Kaatz, P.; Shelton, D. P. *Opt. Commun.* **1998**, 157, 177-181.

(13) Kazjar, F.; Ledoux-Rak, I.; Zyss, J. *Phys. Rev. A.*, **1987**, 36, 2210-2219.

(14) Teng, C. C.; Man, H. T. *Appl. Phys. Lett.* **1990**, 56, 1734-1736.

List of References

1. Ahlheim, M.; Barzoukas, M.; Besworth, P. V.; Blanchard-Desce, F. A.; Hu, Z.-Y.; Marder, S. R.; Perry, J. W.; Runser, C.; Staehelin, M.; Zysset, B. *Science* **1996**, 271, 335-337

2. Akahori, K.; Nishikuri, M.; Nakamatsu, T.: JP 60156760, 1985, p 9.

3. Bella, S. D.; Fragala, I.; Ratner, M. A.; Marks, T. J. *Chem. Mater.* **1995**, 7, 400-404.

4. Bellamy, F. D.; Ou, K. *Tet. Lett.* **1984**, 25, 839-842.

5. Boldt, P.; Eisentrager, T.; Glania, C.; Goldenitz, J.; Kramer, P.; Matschiner, R.; Rase, J.; Schwesinger, R.; Wichern, J.; Wortmann, R. *Adv. Mater.* **1996**, 8, 672-675.

6. Brasselet, S.; Cherioux, F.; Audebert, P.; Zyss, J. *Chem. Mater.* **1999**, 11, 1915-1920.

7. Bredas, J. L.; Adant, C.; Tackx, P.; Persoons, A.; Pierce, B. M. *Chem. Rev.* **1994**, 94, 243-276.

8. Burland, D. M.; Miller, R. D.; Reiser, O.; Tweig, R. J.; Walsh, C. A. *J. Appl. Phys.* **1992**, 71, 410-417.

9. Champagne, B.; Kirtman, B. *Chem. Phys.* **1999**, 245, 213-226.

10. Cheng, L.-T.; Tam, W.; Stevenson, S. H.; Meredith, G. R.; Rikken, G.; Marder, S. R. *J. Phys. Chem.* **1991**, 10631-10643.

11. Cheng, L.-T.; Tam, W.; Marder, S. R.; Steigman, A. E.; Rikken, G.; Spangler, C. W. *J. Phys. Chem.* **1991**, 95, 10643-10653.

12. Cho, B. R.; Son, K. N.; Lee, S. J.; Kang, T. I.; Han, M. S.; Jeon, S. J. *Tetrahedron Lett.* **1998**, 39, 3167-3170.

13. Chou, S.-S.; Hsu, G.-T.; Lin, H.-C. *Tetrahedron Lett.* **1999**, 40, 2157-2160.

14. Clays, K.; Persoons, A. *Phys. Rev. Lett.* **1991**, 66, 2980-2983.

15. Dalton, L. R. *Adv. Polym. Sci.* **2002**, 158, 1-68

16. Dalton, L. R.; Harper, A. W.; Robinson, B. H. *Proc. Natl. Acad. Sci.* **1997**, 94, 4842-4847.

17. Dalton, L. R.; Harper, A. W.; Ghosn, R.; Steier, W.; Ziarim, M.; Fetterman, H. R.; Shi, Y.; Mustacich, R. V.; Jen, A. K.-Y.; Shea, K. J. *Chem. Mater.* **1995**, 7, 1060-1081.

18. Dalton, L. R.; Sapochak, L. S.; Yu, L. *J. Phys. Chem.* **1993**, 97, 2871-2883.

19. Dalton, L. R.; Steier, W.; Robinson, B. H.; Zhang, C.; Ren, A.; Garner, S.; Chen, A.; Londergan, T.; Irwin, L.; Carlson, B.; Fifield, L.; Phelan, G.; Kincaid, C.; Amend, J.; Jen, A. K.-Y. *Mater. Chem.* **1999**, 9, 1905-1920.

20. Dalton, L. R. *Nature* **1992**, 359, 269.

21. Dalton, L. R.; Harper, A. W. *Polym. News*, **1998**, 23, 114-120.

22. Firestone, K. A.; Reid, P. J.; Lawson, R.; Jang, S.-H.; Dalton, L. R. *Inorg. Chim. Acta.* **2004**, 357, 3957-3966.

23. Firestone, K. A., personal communication

24. Franken, P. A.; Hill, A. E.; Peters, C. W.; Weinreich, G. *Phys. Rev. Lett.* **1961**, 7, 118-120.

25. Haller, M.; Luo, J.; Li, H.; Kim, T.-D.; Liao, Y.; Robinson, B. H.; Dalton, L. R.; Jen, A. K.-Y. *Macromolecules*, **2004**, 37, 688-690.

26. Harper, A. W.; Sun, S.; Dalton, L. R.; Garner, S. M.; Chen, A.; Kalluri, S.; Steier, W. H. *J. Opt. Soc. Am. B: Opt. Phys.* **1998**, 15, 329-337.
He, M.; Leslie, T.; Sinicropi, J. A. *Chem. Comm.* **2002**, 14, 2393-2400.

27. Illien, B.; Jehan, P.; Botrel, A.; Darchen, A.; Ledoux-Rak, I.; Zyss, J.; Lahcene, O. *New J. Chem.* **1998**, 22, 633-641.

28. Isobe, T.; Fukuda, K.; Ishikawa, T. *Tetrahedron: Asymmetry*, **1998**, 9, 1729-1735.

29. Jang, S. H., personal communication

30. Jen, A. K.-Y.; Rao, V. P.; Wong, K. Y.; Drost, K. J. *J. Chem. Soc., Chem. Commun.* **1993**, 90-92.

31. Jen, A. K.-Y.; Rao, V. P.; Drost, K. J.; Wong, K. Y.; Cava, M. P. *J. Chem. Soc., Chem. Commun.* **1994**, 2057-2059.

32. Jen, A. K.-Y.; Wong, K. Y.; Rao, V. P.; Drost, K. J.; Cai, Y. M. *J. Electron. Mater.* **1994**, 23, 653-657.

33. Jen, A. K.-Y., personal communication

34. Kaatz, P.; Shelton, D. P. *Opt. Commun.* **1998**, 157, 177-181.

35. Karna, S. P.; Zhang, Y.; Samoc, M.; Prasad, P. N.; Reinhardt, B. A.; Dillard, A. G. *J. Chem. Phys.* **1993**, 99, 9984-9993.

36. Katti, K. V.; Raghuraman, K.; Pillarsetty, N.; Karra, S. R.; Gulotty, R. J.; Chartier, M. A.; Langhoff, C. A. *Chem. Mater.* **2002**, 14, 2436-2438.

37. Katz, H. E.; Singer, K. D.; Sohn, J. E.; Dirk, C. W.; King, L. A.; Gordon, H. M. *J. Amer. Chem. Soc.* **1987**, 109, 6561-6563.

38. Kazjar, F.; Ledoux-Rak, I.; Zyss, J. *Phys. Rev. A.*, **1987**, 36, 2210-2219.

39. Kofron, W. G.; Baclawski, L. M. *J. Org. Chem.* **1976**, 41, 1879-1880.

40. Lalama, S. J.; Garito, A. F. *Phys. Rev. A: At. Mol. Opt. Phys.* **1979**, 20, 1179-1194.

41. Levine, B. F.; Bethea, C. G. *J. Chem. Phys.* **1977**, 66, 1070-1074.

42. Lipinski, J.; Bartkowiak, W. *Chem. Phys.* **1999**, 245, 263-276.

43. Liu, S.; Haller, M.; Ma, H.; Dalton, L. R.; Jang, S.-H.; Jen, A. K.-Y. *Adv. Mater.* **2003**, 15, 603-607.

44. Londergan, T.; Zhang, C.; Ren, A.; Dalton, L. R. *Polym. Prepr. (Am. Chem. Soc. Div. Polym. Chem.)* **2000**, 41, 783-784.

45. Luo, J.; Liu, S.; Haller, M.; Liu, L.; Ma, H.; Jen, A. K.-Y. *Adv. Mater.* **2002**, 14, 1763-1768.

46. Luo, J.; Ma, H.; Haller, M.; Jen, A. K.-Y.; Barto, R. R. *Chem. Comm.* **2002**, 888-889.

47. Ma, H.; Liu, S.; Luo, J.; Suresh, S.; Liu, L.; Kang, S. H.; Haller, M.; Sassa, T.; Dalton, L. R.; Jen, A. K.-Y. *Adv. Funct. Mater.* **2002**, 12, 565-574.

48. Marder, S. R.; Cheng, L.-P.; Tiemann, B. G.; Friedli, A. C.; Blanchard-Desce, M.; Perry, J. W.; Runser, C.; Staehelin, M.; Zysset, B. *Science*, **1994**, 263, 511-514.

49. Marder, S. R.; Gorman, C. B.; Meyers, F.; Perry, J. W.; Bourhill, G.; Bredas, J. L.; Pierce, B. M. *Science*, **1994**, 265, 632-635.

50. Marder, S. R.; Perry, J. W. *Science*, **1994**, 263, 1706-1707.

51. Melikian, G.; Rouessac, F. P.; Alexandre, C. *Synth. Comm.* **1995**, 25, 3045-3051.

52. Moylan, C. R.; Tweig, R. J.; Vee, V. Y.; Swanson, S. A.; Betterton, K. M.; Miller, R. D. *J. Am. Chem. Soc.* **1993**, 115, 12599-12600.

53. Nie, W. *Adv. Mater.* **1993**, 5, 520-545.

54. Oudar, J. L.; Chemla, D. S. *J. Chem. Phys.* **1977**, 66, 2664-2668.

55. Painelli, A. *Chem. Phys.* **1999**, 245, 185-197.

56. Prasad, P. N.; Williams, D. J. *Introduction to Nonlinear Optical Effects in Molecules and Polymers*; John Wiley and Sons: New York, **1991**.

57. Raimundo, J.-M.; Blanchard, P.; Gallego-Planas, N.; Mercier, N.; Ledoux-Rak, I.; Hierle, R.; Roncali, J. *J. Org. Chem.* **2002**, 67, 205-218.

58. Rao, V. P.; Jen, A. K.-Y.; Chandrasekhar, J.; Namboothiri, I. N. N.; Rathna, A. *J. Am. Chem. Soc.* **1996**, 118, 12443-12448.

59. Rao, V. P.; Wong, K. Y.; Jen, A. K.-Y.; Drost, K. J. *Chem. Mater.* **1994**, 6, 2210-2212.

60. Rao, V. P.; Cai, Y. M.; Jen, A. K.-Y. *J. Chem. Soc., Chem. Commun.* **1994**, 1689-1690.

61. Rao, V. P.; Jen, A. K.-Y.; Wong, K. Y.; Drost, K. J. *Tetrahedron Lett.* **1993**, 34, 1747-1750.

62. Shen, Y. R. *The Principles of Nonlinear Optics*; John Wiley and Sons: New York, **1984**.

63. Singer, K. D.; Sohn, J. E.; King, L. A.; Gordon, H. M.; Katz, H. E.; Dirk, C. W. *J. Opt. Soc. Am. B: Opt. Phys.* **1989**, 6, 1339-1350.

64. Song, S.; Lee, S. J.; Cho, B. R. *Chem. Mater.* **1999**, 11, 1406-1408.

65. Steier, W. H.; Chen, A.; Lee, S. S.; Garner, S.; Zhang, H.; Chuyanov, V.; Dalton, L. R.; Wang, F.; Ren, A.; Zhang, C.; Todorova, G.; Harper, A. W.; Fetterman, H. R.; Chen, D.; Udupa, A.; Bhattacharya, D.; Tsap, B. *Chem. Phys.* **1999**, 245, 487-506.

66. Teng, C. C.; Man, H. T. *Appl. Phys. Lett.* **1990**, 56, 1734-1736.

67. Tretiak, S.; Chemnyak, V.; Mukamel, S. *Chem. Phys.* **1999**, 245, 145-163.

68. van der Boom, M. E.; Zhu, P.; Evmenenko, G.; Malinsky, J. E.; Lin, W. D.; Marks, T. J. *Langmuir*, **2002**, 18, 3704-3707.

69. van der Boom, M. E.; Evmenenko, G.; Dutta, P.; Marks, T. J. *Mater. Sci. Eng.* **2002**, 375-376.

70. Williams, D. J. *Angew. Chem. Int. Ed.* **1984**, 23, 690-703.

71. Wong, K. Y.; Jen, A. K.-Y.; Rao, V. P.; Drost, K. J. *J. Chem. Phys.* **1994**, 100, 6818-6825.

72. Xu, C.; Wu, B.; Todorova, G.; Dalton, L. R.; Shi, Y.; Ranon, P. M.; Steier, W. H. *Macromolecules*, **1993**, 26, 5303-5309.

73. Zhang, C.; Fetterman, H. R.; Steier, W.; Michael, J.: US 6347992, 2001, p 33.

Appendix A: Acceptor Research

Section 1: Previous TCF Research

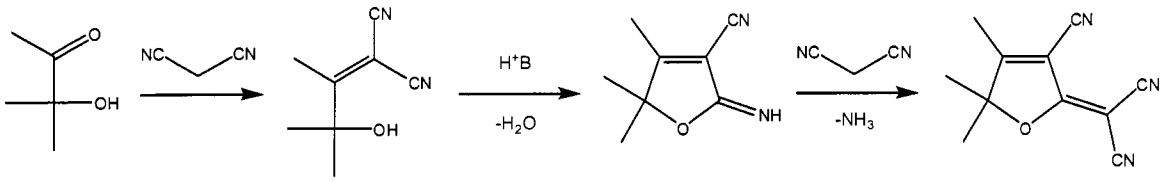

12 13 TCF

Figure A.1 Synthesis of the TCF acceptor

The TCF acceptor was discovered in 1995 and set a new standard for performance, ease of synthesis and stability.[1] This acceptor is prepared by reacting malononitrile with 3-hydroxy-3-methyl-2-butanone in ethanol in the presence of base as shown in Figure A.1. The proposed mechanism involves condensation of malononitrile with the ketone of 3-hydroxy-3-methyl-2-butanone to form compound **12** which then cyclizes to form imine **13**. This imine reacts with another malononitrile molecule to create the TCF acceptor. When microwave chemistry was employed to optimize this reaction, the imine was isolated, supporting the proposed mechanism.[2]

Section 2: Attempts to vary Electron-Withdrawing Groups

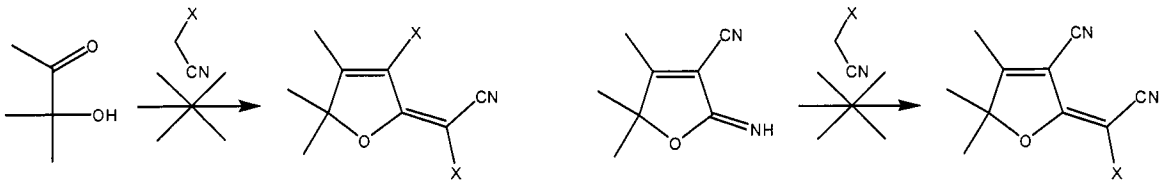

X = SO_2CF_3, NO_2, $COCF_3$, SO_2CH_3

Figure A.2 Attempts at generating TCF-type acceptors with more powerful electron-withdrawing groups

A host of electron-withdrawing groups with greater potency than cyano exist and exploration of these groups is the most obvious method by which to generate more powerful acceptors. Nitro, trifluoromethylsulfonyl, trifluoromethylacetate and methylsulfonyl acetonitriles where prepared and reacted with 3-hydroxy-3-methyl-2-butanone under a wide array of conditions both conventional and microwave initiated as illustrated in Figure A.2. Neither acid nor base catalysts resulted in formation of the desired product. Imine formation appears to be delicate electronically and sterically so imine **13** was prepared using a microwave reactor and isolated via silica-gel chromatography. All attempts a reacting the various acetonitriles with imine **13** resulted in failure. After an exhaustive search for conditions that would facilitate the desired reaction, it was theorized that use of more powerful electron-withdrawing groups stabilizes the anion reducing its nucleophilicity such that condensation fails to proceed as shown in Figure A.3.

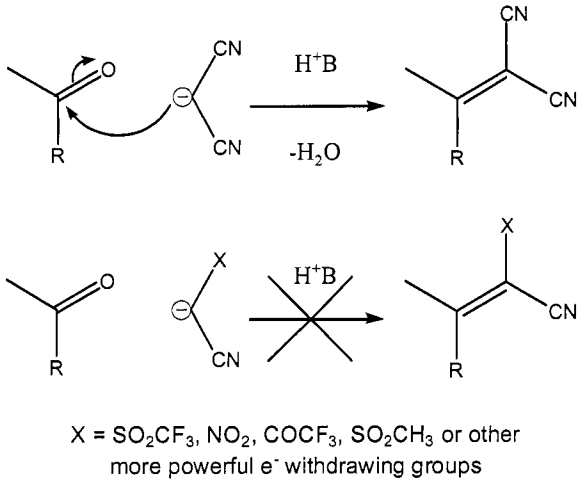

Figure A.3 Explanation for failure of more powerful electron-withdrawing group investigation

Section 3: Previous TCF-CF_3 Research

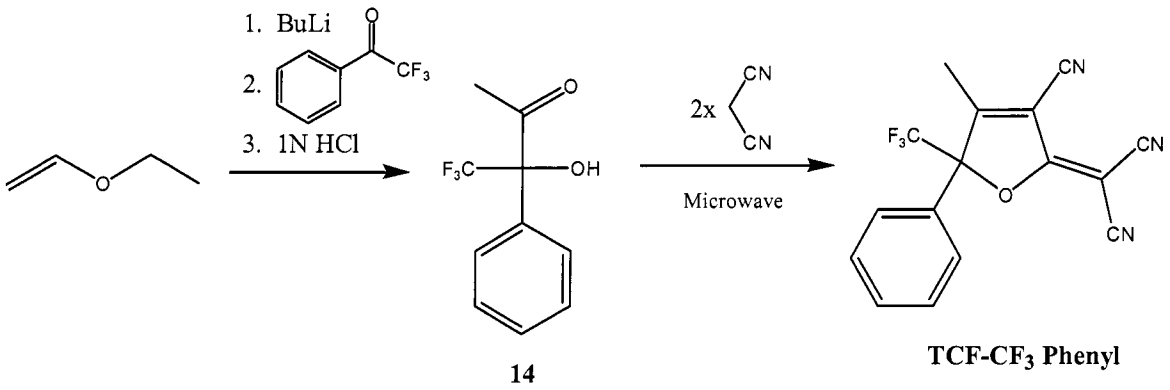

Figure A.4 Synthesis of TCF-CF_3 acceptors

Although attempts at modification of TCF through use of more potent electron-withdrawing groups failed, adjustment of the peripheral functionalities has lead to some surprising result.[3] Jen and coworkers discovered that replacement of one of the methyl

groups with trifluoromethyl results in a dramatic increase in chromophore β value.[2-4] The enhanced performance of the TCF-CF_3 acceptor comes at the price of reduced stability, increased synthetic difficulty and the need for microwave chemistry to achieve good yields.[2] The synthesis of the TCF-CF_3 phenyl acceptor was developed by Yi Liao in the Dalton group and is illustrated in Figure A.4. Despite these issues, TCF-CF_3 materials have become the new work-horse acceptors.

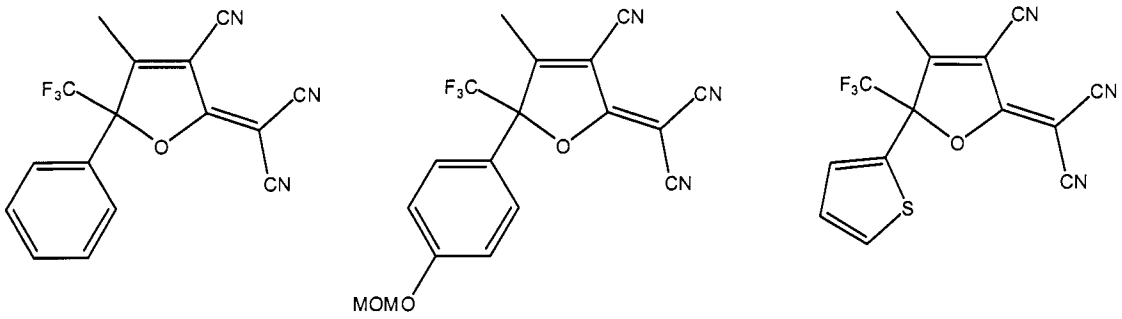

TCF-CF_3 Phenyl **TCF-CF_3 MOM-Phenyl** **TCF-CF_3 Thiophene**

Figure A.5 The TCF-CF_3 phenyl acceptor as well as the more powerful TCF-CF_3 MOM-phenyl and TCF-CF_3 thiophene acceptors

Section 4: Attempts to vary TCF-CF_3 Functionality

It was noted that data suggests that the TCF-CF_3 MOM-phenyl and TCF-CF_3 thiophene acceptors, synthesized by the Jen Group and shown in Figure A.5, are marginally more powerful than the TCF-CF_3 phenyl acceptor.[5] The curious interplay between electron-richness at the location adjacent to CF_3 inspired further investigation. Compounds **15**, **16** and **17** (Figure A.6) were targeted to determine if placement of highly

electron-rich structures adjacent to CF_3 would further enhance chromophore β value. Synthesis began by reacting compounds **18**, **19** and **20** with *n*-BuLi and ethyl trifluoroacetate to generate compounds **21**, **22** and **23** which where then reacted with lithiated ethylvinyl ether. Compounds **24** and **25** were unstable and decomposed, but compound **26** was stable and was isolated by silica-gel chromatography. Compound **26** was reacted with malononitrile under a variety of conditions, but acceptor **17** was not detected.

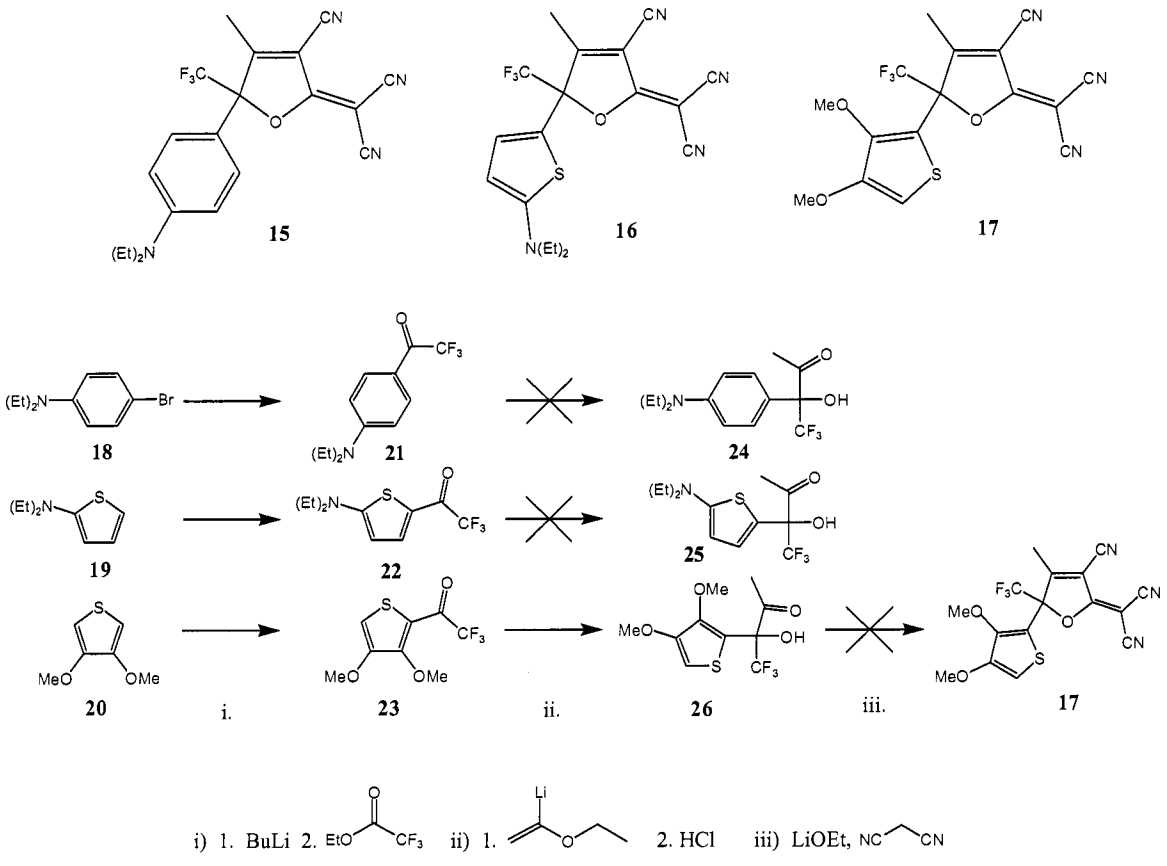

Figure A.6 Proposed TCF-CF_3 acceptors and their synthesis

Section 5: Previous TCP Research

Tricyano-pyrrilidone (TCP) acceptors have been used in textile dyes for over 20 years, but their usage in NLO chromophores was explored relatively recently by the Jen and Dalton groups.[6] These acceptors are fairly robust and significantly more powerful than both TCF and TCF-CF_3 acceptors, but unfortunately their extremely planar nature inhibits translation of excellent chromophore β to high r_{33} values most likely due to chromophore aggregation issues.[7] Additionally, the acceptor is generally linked to chromophores by reaction of chloro-TCP with the donor bridge because of synthetic issues unique to the TCP acceptor.[7] Chloro-TCP is quite reactive and consequently this methodology is only applicable to a relatively small range of systems that posses adequate stability to survive the reaction conditions.

Section 6: Attempts to generate Six-Membered TCP Acceptors

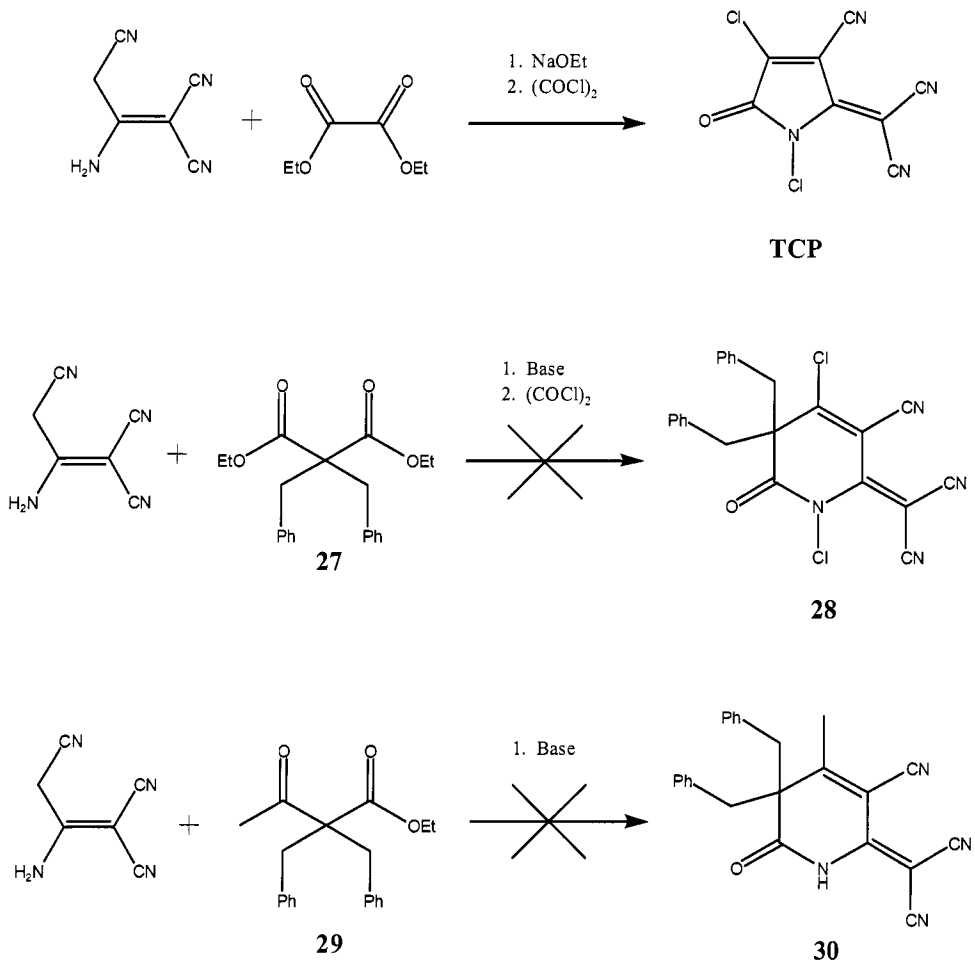

Figure A.7 Synthesis of TCP and attempts at synthesisizing modified versions

The decision was made to modify TCP to reduce its planarity and hopefully increase the performance of materials containing TCP-based chromophores. The synthesis of chloro-TCP is illustrated in Figure A.7. Increasing the size of the ring from 5 members to 6 allows for functionalization with bulky groups. Compound **27** was prepared by reaction of the corresponding diester with sodium hydride and benzyl

bromide. The diester was then reacted with 2-amino-1-propene-1,1,3-tricarbonitrile under a variety of conditions including standard TCP synthetic conditions, but acceptor **28** could not be generated. Esters generally do not readily undergo the necessary condensation reactions, however TCP is generated from diethyl oxalate in which the esters are adjacent to each other. The proximity of these esters likely activates them facilitating the reaction while in compound **27** the esters are isolated from each other electronically. Compound **29** was generated by reacting ethyl-acetoacetate with sodium hydride and benzyl bromide. It was hoped that successful reaction of compound **29** with 2-amino-1-propene-1,1,3-tricarbonitrile would result in condensation with the ketone and subsequently ring closure through amide generation to form acceptor **30**. A variety of conditions were explored, but acceptor **30** was not isolated.

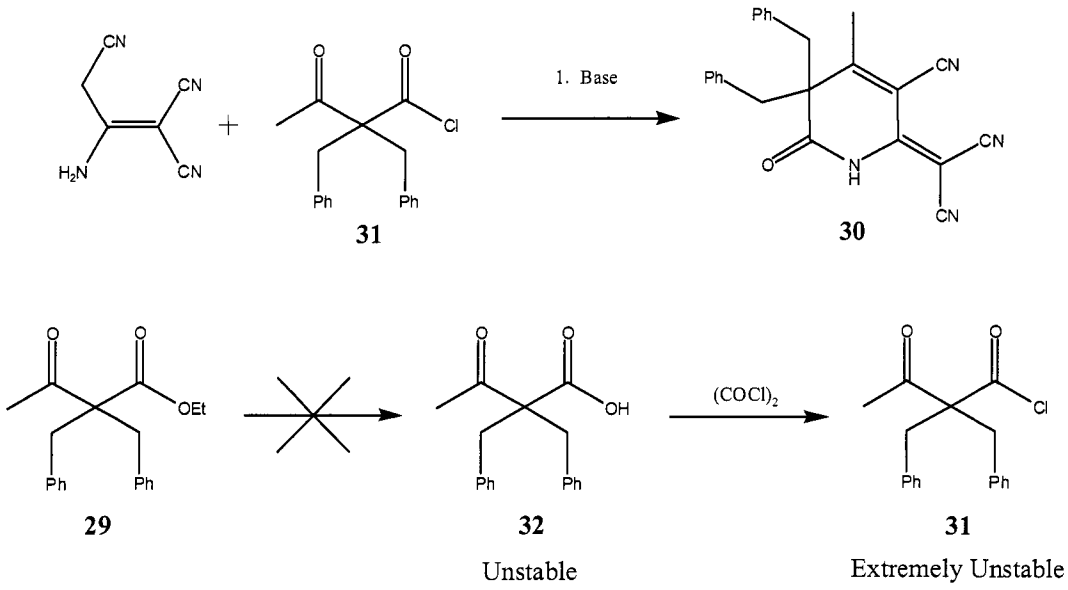

Figure A.8 Attempted synthesis via acid chloride

A revised scheme for generation of acceptor **30** via the acid chloride is illustrated in Figure A.8. Reaction of acid chloride **31** with 2-amino-1-propene-1,1,3-tricarbonitrile should form an amide, which could intramolecularly condense to form acceptor **30**. Generation of the carboxylic acid **32** from ester **29** proved to be far more difficult than expected. A wide variety of conditions were explored including trimethylsilyl iodide and various acidic and basic conditions, but deprotection without decarboxylation was not achieved. Work began to explore more labile protecting groups that could be cleaved without decarboxylation, but was abandoned when a reference was located indicating the extreme instability of acid chloride **31**.[8]

Section 7: Attempts to Generate Acceptors with Expanded Conjugation

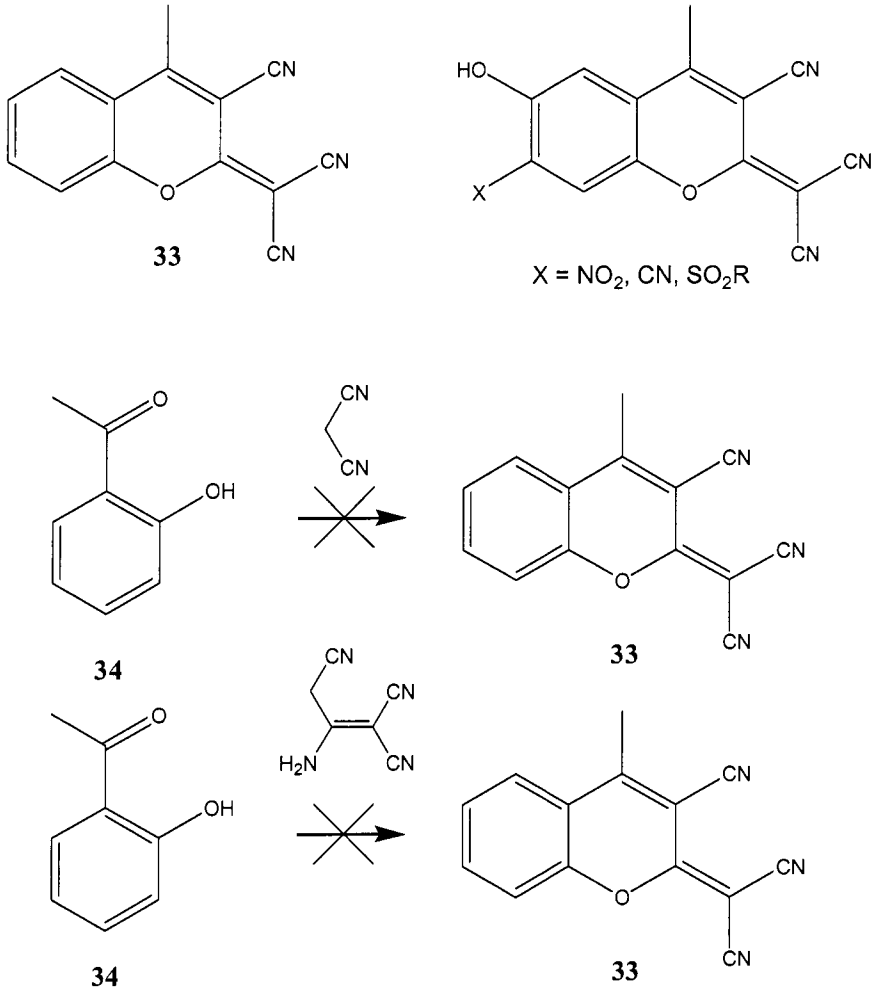

Figure A.9 Acceptors with expanded conjugation

The increased power of the TCF-CF_3 and TCP acceptors compared to TCF is not entirely understood. One possible explanation is that conjugation of TCP's carbonyl and hyper-conjugation of TCF-CF_3's trifluoromethyl allow further delocalization of charge and stabilize charge-separated chromophore states.[5,7] If this explanation has merit,

synthesis of acceptors with expanded conjugation should yield increased strength. Acceptor **33** was chosen as a target molecule because it is synthesizable from commercially available materials, with the ultimate goal being generation of acceptors with phenols for functionalization and further electron-withdrawing groups as shown in Figure A.13. Attempts at condensing compound **34** with malononitrile resulted in dimerized and oligomerized ketone. Figure A.1 illustrates the synthesis of the TCF acceptor and provides some insight into the dynamics of its formation. Compound **12** cannot be isolated suggesting that its formation is a rate limiting step. This condensation is likely highly reversible, and if cyclization to generate imine does not proceed readily, competition with starting material dimerization becomes significant. It is probable that the phenol, particularly when in conjugation with the cyano groups, is not nucleophilic enough to undergo imine formation. Numerous attempts to react compound **34** with 2-amino-1-propene-1,1,3-tricarbonitrile also failed to produce product.

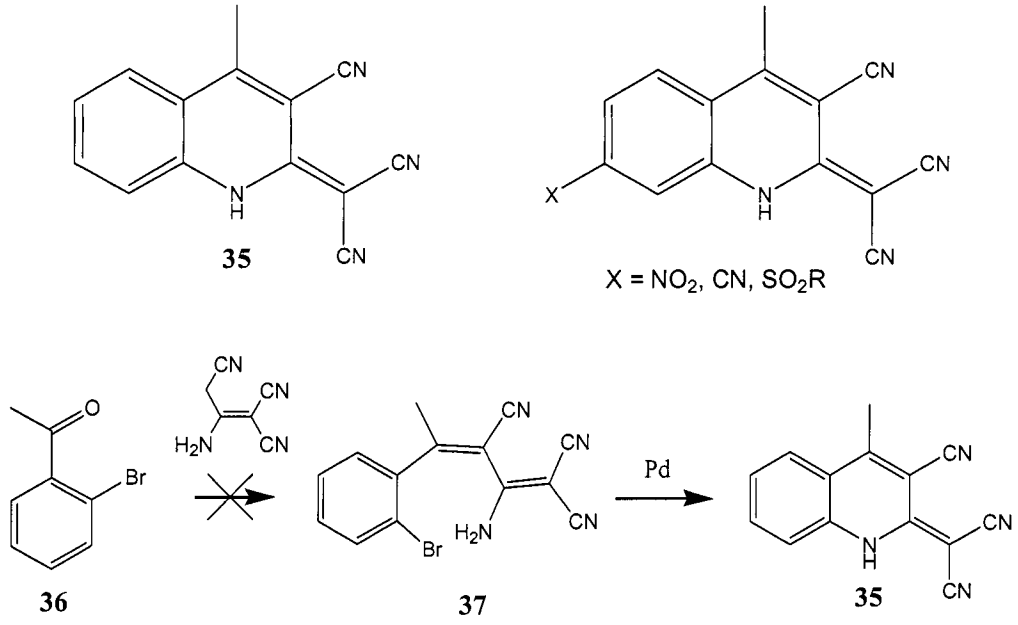

Figure A.10 Alternative route to acceptors with expanded conjugation

Acceptor **35** was chosen as a new target molecule in hopes that reaction of compound **36** with 2-amino-1-propene-1,1,3-tricarbonitrile would result in generation of compound **37**, which could then be cyclized using a Pd as shown in Figure A.14. Acceptor **35** possess an amine that could serve as a functionalization point and other acceptors with further electron-withdrawing groups could be generated through similar chemistry. Numerous attempts were made to generate compound **37**, but it could not be synthesized in appreciable amounts due to difficulties in achieving condensation and so dimerization of the starting materials was the dominant reaction.

Section 8: Previous TCNQ Research

7,7,8,8-tetracyanoquinodimethane (TCNQ) is a very powerful acceptor that has been used extensively in organic conductors. To a lesser degree TCNQ has been explored as an acceptor in NLO chromophores. There are two major issues preventing success of these chromophores in EO materials. Firstly, chromophores containing TCNQ are generally zwitterionic due to power of this acceptor, which leads to issues with aggregations, solubility, purification and transparency to telecommunication wavelengths. The second major issue with the TCNQ acceptor is its extremely planar nature that further exasperates issues of solubility and aggregation resulting in poling difficulties.

Section 9: Attempts at generating Functionalized TCNQ's

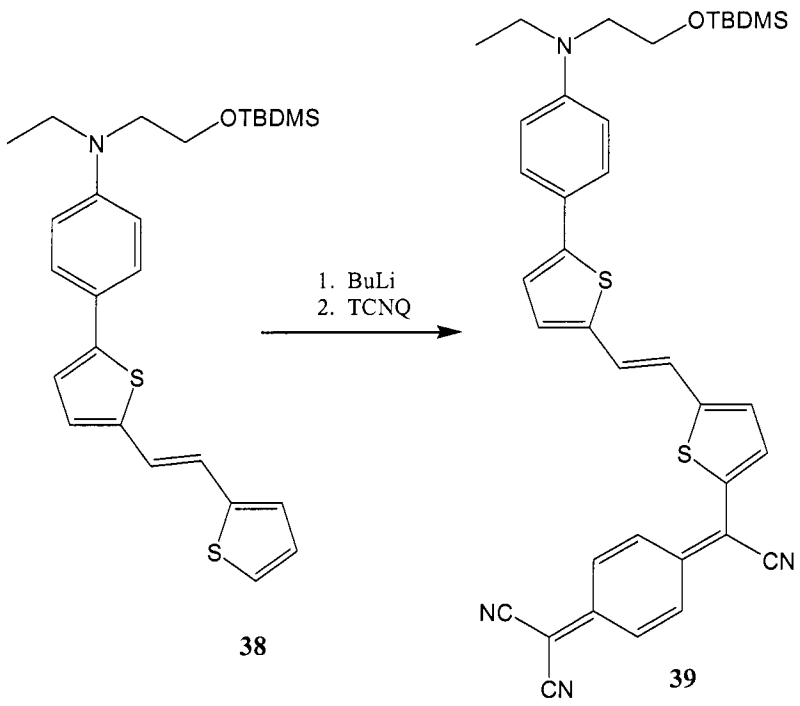

38 39

Figure A.11 Generation of TCNQ-containing chromophore

Theoretically, by increasing the bridge length to separate charges and increasing bridge aromaticity, it should be possible to generate TCNQ chromophores with neutral ground states. Figure A.9 illustrates the synthesis of an extended TCNQ chromophore. Literature preparations for shorter chromophores involve heating donor-bridge with TCNQ. However, this methodology does not work for extended systems. Compound **38** is reacted with *n*-BuLi and subsequently with TCNQ to generate chromophore **39**. This chromophore displays a λ_{max} of 849 nm in chloroform and 782 nm in dioxane. The direction of solvatochromism confirms that chromophore **39** does indeed possess a

neutral ground state and to the author's knowledge is the first TCNQ chromophore that is not zwitterionic.

With ability to generate non-zwitterionic TCNQ chromophores established, the decision was made to generate functionalized TCNQ's in hopes of generating chromophores for high r_{33} materials. The commercial availability of compound **41** inspired generation of the two functionalized acceptors depicted in Figure A.9. Acceptor **42** was generated through an efficient one-pot reaction with dendron **40**. Acceptor **43** was generated cleanly by reaction of compound **41** with DHP.

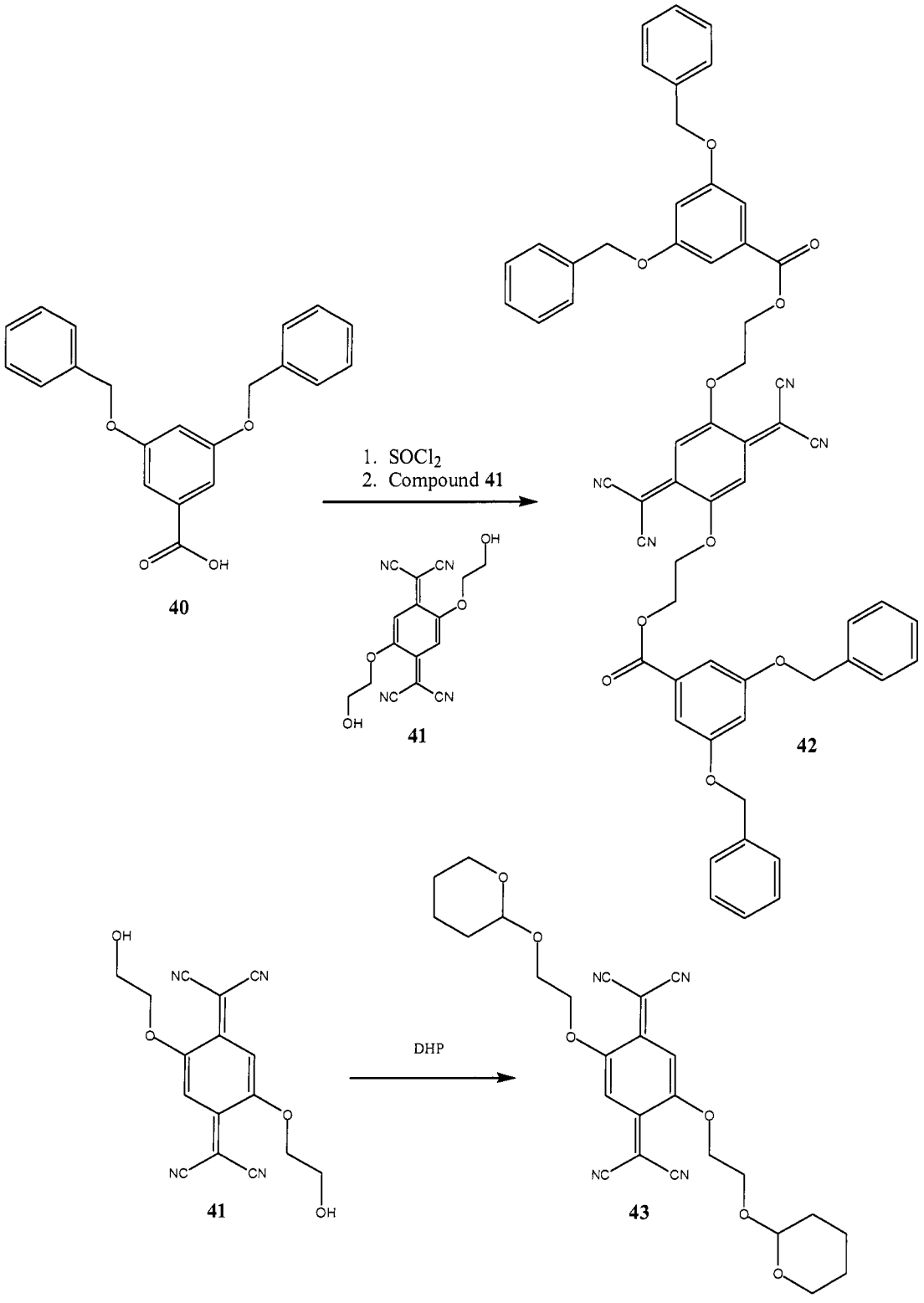

Figure A.12 Synthesis of functionalized TCNQ's

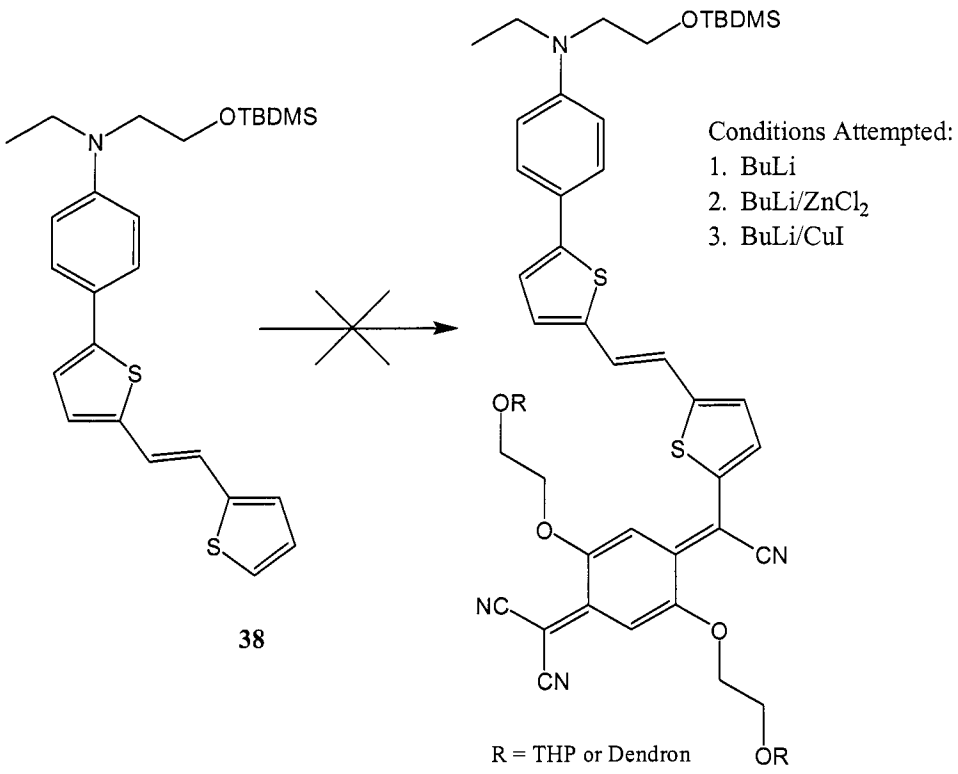

Figure A.13 Attempts to link functionalized TCNQ's to compound 38

Although attachment of TCNQ to compound **38** proceeded efficiently with *n*-BuLi, attachment of acceptors **42** and **43** failed under similar conditions. An array of conditions and coupling intermediates were explored (Figure A.11) in an effort to achieve linkage of the acceptors to the donor bridge, but all failed. Although acceptor **42** is fairly sterically hindered, acceptor **43** is not particularly hindered, suggesting that the difference in reactivity between the functionalized TCNQ's and standard TCNQ is likely electronic rather than steric in nature. It is possible that the oxygens in conjugation with the TCNQ

ring increase electron richness sufficiently that they reduce the electrophilicity sufficiently to inhibit reaction.

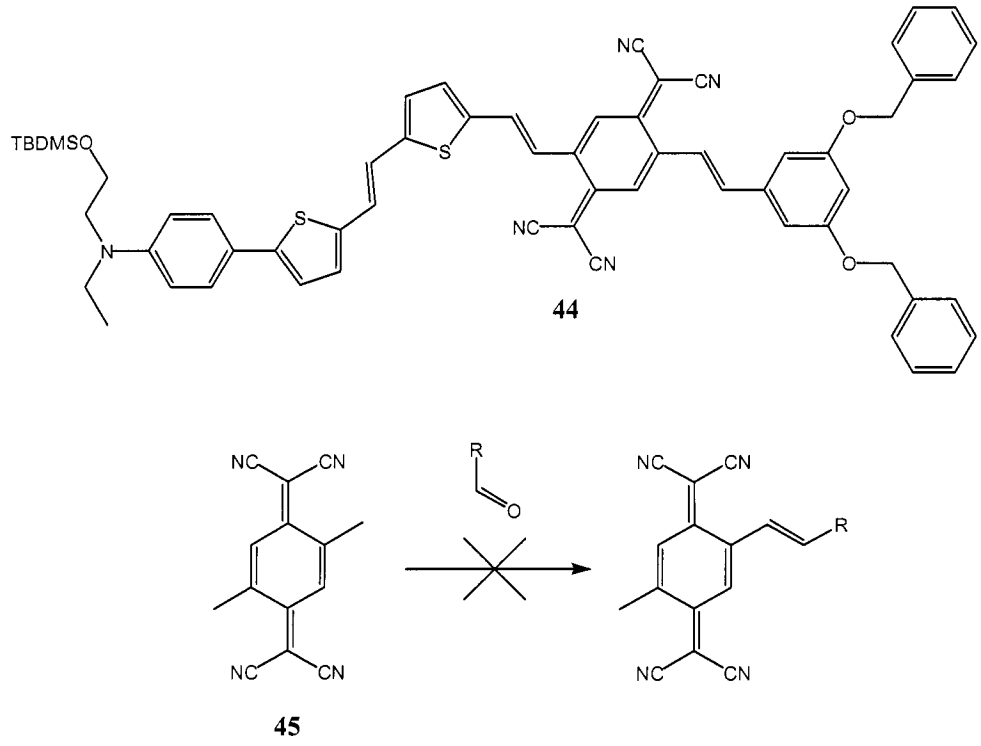

Figure A.14 Dimethyl-TCNQ Acceptor

It was noted that compound **45** (Figure A.12) was commercially available and appeared to offer the possibility of functionalized TCNQ's without problematic ethers. The methyl groups of compound **45** should be highly acidic due to the cyano functionalities and could undergo condensation reactions with aldehydes allowing for linkage to donor bridge aldehydes or bulky groups to prevent aggregation. Theoretically, compound **45** could be reacted with two dendron-aldehydes and then attached to the

chromophore similarly to TCNQ or compound **45** could be condensed with a donor-bridge-aldehyde and dendron to make molecules similar to compound **44**. Unfortunately, attempts at achieving condensation under acid and based catalyzed conditions resulted in failure. The methyl groups do not appear to readily undergo condensation reactions to an appreciable degree.

Section 10: Conclusion

Synthesis of new acceptors has been an area of intense study in the Dalton and Jen groups as well as many other organizations researching NLO chromophores. Discovering stable and synthetically accessible acceptors that perform well in materials has proven to be an exceedingly challenging task. The TCF acceptor was discover by chance over a decade ago.[1] After roughly five years of attempts to improve its performance, the TCF-CF_3 acceptors were discovered.[3] Since their development, no significant improvements to acceptors have been made despite years of investigation by dozens of researchers. The field of acceptors will continue to confound researchers as the discovery of the next workhorse acceptor promises to push the EO field to a new plateau in performance.

Notes to Appendix A

(1) Melikian, G.; Rouessac, F. P.; Alexandre, C. *Synth. Comm.* **1995**, 25, 3045-3051.

(2) Liu, S.; Haller, M.; Ma, H.; Dalton, L. R.; Jang, S.-H.; Jen, A. K.-Y. *Adv. Mater.* **2003**, 15, 603-607.

(3) Zhang, C.; Fetterman, H. R.; Steier, W.; Michael, J.: US 6347992, 2001, p 33.

(4) He, M.; Leslie, T.; Sinicropi, J. A. *Chem. Comm.* **2002**, 14, 2393-2400.

(5) Jen, A. K.-Y., personal communication

(6) Akahori, K.; Nishikuri, M.; Nakamatsu, T.: JP 60156760, 1985, p 9.

(7) Jang, S. H., personal communication

(8) Olah, G. A.; Kuhn, S. J. *J. Org. Chem.* **1961**, 26, 225-227.

Vita

Nicholas Buker grew up in Burlington ,Vermont. He attended the University of Vermont were he obtained his BS in Chemistry in 1999. From 1999 until 2000 he worked at International Business Machines (IBM) doing process development for semiconductor fabrication. In 2000 he moved to Seattle to attend the University of Washington and pursue his PhD in Chemistry.